Charged clusters in thin film growth

Nong-Moon Hwang*[1] and Doh-Yeon Kim[1]

A cauliflower structure is a granular film composed of spherical particles similar in size, each with numerous nanoscale nodules on its surface. The structure is produced during certain chemical vapour deposition (CVD) processes for diamond and silicon thin film growth. A classical account in terms of atomic unit deposition fails to explain the growth of such a cauliflower structure, as it requires a gas phase of much higher supersaturation than for onset of diffusion controlled growth. Another interesting and somewhat puzzling phenomenon encountered during a diamond CVD process is that while diamond is depositing on a graphite substrate, carbon atoms in the graphite itself are etched away into the vapour phase; that is, experience evaporation. Again, an elementary kinetic barrier mechanism fails to explain such CVD deposition of a less stable diamond phase combined with simultaneous evaporation of a stable graphite phase. In order to account for such puzzling CVD phenomena and others, a theory of charged clusters has been developed over the past decade as a new paradigm for thin film growth. The theory and its applications are reviewed in this work.

Keywords: Theory of charged clusters, Thin films, Growth mechanism, Chemical vapour deposition (CVD), Physical vapour deposition, Diamond CVD, Silicon CVD

IMR/410

Introduction

It is generally believed that the growth unit of chemical (CVD) and physical (PVD) vapour deposited thin films is either an atom or a molecule. The atom first adsorbs onto the surface on a terrace, diffuses to a ledge, and finally becomes incorporated in the crystal lattice.[1,2] The selective accommodation of atoms at the kink results in atomic self-assembly, which produces a crystal structure with regular arrays of atoms. Without atomic self-assembly, the film would be amorphous.

A drastically different thin film growth mechanism is suggested in the theory of charged clusters (TCC).[3–5] According to this theory, charged clusters form in the gas phase with their subsequent deposition as films in many thin film processes, where the films were previously believed to grow by an individual atom or molecule. If clusters are neutral, they undergo random Brownian coagulation, leading to a porous skeletal structure. If clusters are charged (normally singly charged), however, they undergo orderly packing or self-assembly, leading to void-free dense films. For deposition of insulating materials, the electric charge built up on the growing surface should be removed, which is achieved usually by surface ionisation[6] of the gas species in the thin film reactor. Perfection of growing films increases with decreasing cluster size, because smaller clusters are favourable for epitaxial recrystallisation upon landing on a growing surface. As the cluster size increases or the substrate temperature decreases, defects such as twins or grain boundaries tend to form.[3,7]

In this new paradigm of thin film growth in most CVD and some PVD processes, important parameters are the cluster size and its charging behaviour, which are affected by the work function of the heated surface, flowrate of precursor, carrier gas, temperature and pressure. Charging of clusters can be easily understood in the thin film process adopting plasma. The main mechanism of cluster charging in the non-plasma process turned out to be surface ionisation described by the Saha–Langmuir equation.[8] Charged clusters are formed in one of two ways. In the first case, gas atoms or molecules undergo surface ionisation on the heated surface and become ionised. The resultant ions act as a centre for nucleation, forming charged clusters.[9,10] In the second case, clusters are formed first and these clusters undergo surface ionisation on a heated surface.[11,12]

The TCC was developed while studying the growth mechanism of CVD diamond. Many puzzling phenomena in the process were explained by the new theory.[3,13,14] Most importantly, the so-called thermodynamic paradox of diamond deposition and simultaneous graphite etching[15] was successfully explained without violating the second law of thermodynamics.[13] The existence of hypothetical negatively charged clusters containing hundreds of carbon atoms was experimentally confirmed.[16–18] It was shown that the cluster size increased with increasing methane concentration. Small clusters produced high quality diamonds with well defined facets, while large clusters produced poor quality ball-like or cauliflower-shaped diamonds.

The TCC was successfully extended to silicon CVD,[19–22] zirconia CVD,[23,24] and thermal evaporation

[1]Centre for Microstructure Science of Materials, School of Materials Science and Engineering, Seoul National University, Seoul 151–742, Korea

*Corresponding author, email nmhwang@snu.ac.kr

Published by Maney for the Institute of Materials, Minerals and Mining and ASM International
DOI 10.1179/095066004225021891

coating of metals.[11,12,25,26] Based on a morphological analysis of films showing the cauliflower-shaped structure with numerous tiny nanosize nodules and the porous skeletal structure on substrate materials with a high charge transfer rate, thin film growth by charged clusters appears to be general in many thin film processes, including laser ablation and sputtering.[22]

In the previous concept of thin film growth by atomic or molecular units, gas phase nucleation would impose an upper limit on the growth rate because the gas phase nuclei were believed to result in degradation of film quality. However, the growth rate of thin films under the condition where gas phase nucleation is suppressed is impractically low. For example, Adachi and co-workers[27–30] studied systematically the maximum growth rate without gas phase nucleation in atmospheric pressure CVD of SiO_2 using tetraethylorthosilicate. They found that film growth rate was negligible under the condition where gas phase nucleation was suppressed. They measured the number density and size distribution of nanosize particles formed in the gas phase using an optical particle counter and a differential mobility analyser (DMA), respectively. Further, they observed that the growth rate of films increased with increasing number density of clusters in the gas phase.

Because of the impractically low deposition rate without gas phase nucleation as was confirmed by Adachi *et al.*,[29] most thin films in commercial production are being made under the condition where gas phase clustering or nucleation takes place. As long as gas phase nuclei are electrically charged, they do not usually pose any problem in film growth. In order to deposit high quality films at high growth rates, gas phase nucleation should take place and the resultant nuclei should be made electrically charged. In many thin film processes, clusters are spontaneously formed and at the same time spontaneously charged without intentional efforts.

Although there have been many suggestions about growth mechanisms similar to the TCC, they have not been taken seriously in the thin film and crystal growth communities. Sunagawa[31,32] suggested that the growth unit of synthetic diamonds is not an atom, but a much larger unit based on the morphological evolution of synthetic diamonds. Samotoin[33] reported a diamond morphology of spiral growth with a step height of $\sim$8 nm. Based on analysis of this morphology, they suggested that the growth unit of CVD diamond should be clusters commensurable in size with the step height of $\sim$8 nm. Takamura *et al.*[34] investigated the surface morphology of epitaxial $YBa_2Cu_3O_{7-x}$ films prepared by thermal plasma flash evaporation and noted that the main deposition species were clusters ranging in size from 0·3 to 9 nm. The cluster size was measured by the microtrench method.[35] In conformity with the TCC, they observed by scanning tunnelling microscopy (STM) that small 1–2 nm clusters underwent epitaxial spiral growth, medium size 3 nm clusters became epitaxial two-dimensional nuclei, and large clusters over 3 nm produced non-epitaxial island grains.

Glasner and co-workers[36–39] suggested a growth mechanism similar to the TCC during their study on the crystal growth of KBr and KCl in the presence of Pb^{+2} in an aqueous solution. In this case, nanometre sized nuclei are formed in the solution and they become the growth unit. They confirmed the formation of these invisible clusters in the solution by an exothermal peak.[37,39] They showed that an almost perfect crystal grew by orderly packing or self-assembly of these nuclei with crystal perfection increasing with decreasing nuclei size. Based on analysis of scanning electron microscopy (SEM) observations, Ueda *et al.*[40] reported that micrometre sized citric acid monohydrate was crystallised by the regular arrangement of $\sim$60 nm particles.

The purpose of this paper is to review the important aspects of crystal growth by charged clusters. Although this review is focused on thin film growth by charged clusters, crystal growth by charged clusters in solution appears to be an important mechanism also. In this case, only a brief review based on a literature survey is presented.

Generation of charged clusters during thin film processes

Diamond CVD

Background

Since low pressure synthesis of diamond at a relatively high growth rate was demonstrated in the hot filament[41,42] and plasma[43,44] processes, it has been intensively studied. Although the procedure to make diamonds at low pressure is now well established, its underlying principle is not yet understood. It is widely believed that the gas activation process produces atomic hydrogen, although the exact role of the atomic hydrogen is not universally agreed upon.[15,45–47] The most popular explanation was the atomic hydrogen hypothesis,[42] which was based on the fact that atomic hydrogen etches graphite much faster than diamond.[41,48]

The atomic hydrogen hypothesis states that the atomic hydrogen produced by gas activation, such as hot filament and plasma, etches graphite much faster than diamond and therefore metastable diamond can be formed dominantly over stable graphite at low pressure. A simple thermodynamic analysis shows that this statement contradicts the second law of thermodynamics, because less stable diamond should also etch as long as stable graphite etches.[13,15] In other words, diamond cannot deposit under conditions where graphite etches if the deposition unit is an atom. In spite of the critical handicap from the thermodynamic point of view, the atomic hydrogen hypothesis is strongly supported by experimental observation of diamond deposition with simultaneous graphite etching.

This puzzling experimental observation can be explained without violation of the second law of thermodynamics by the TCC, where charged nuclei of carbon are formed in the gas phase with their subsequent deposition as diamond crystals.[3,13,14] Considering the CVD phase diagram of the C–H system, where the carbon solubility in the gas phase increases with decreasing temperature near the substrate temperature, the driving force at the substrate favours etching if gas phase nucleation takes place. Therefore, the puzzling phenomenon can be explained if diamond deposits by a cluster unit and both graphite and diamond etch away simultaneously by an atomic unit.[13]

The TCC explains many other puzzling phenomena of diamond CVD that cannot be explained by the conventional concept of atomic growth.[3,13,14] Of these,

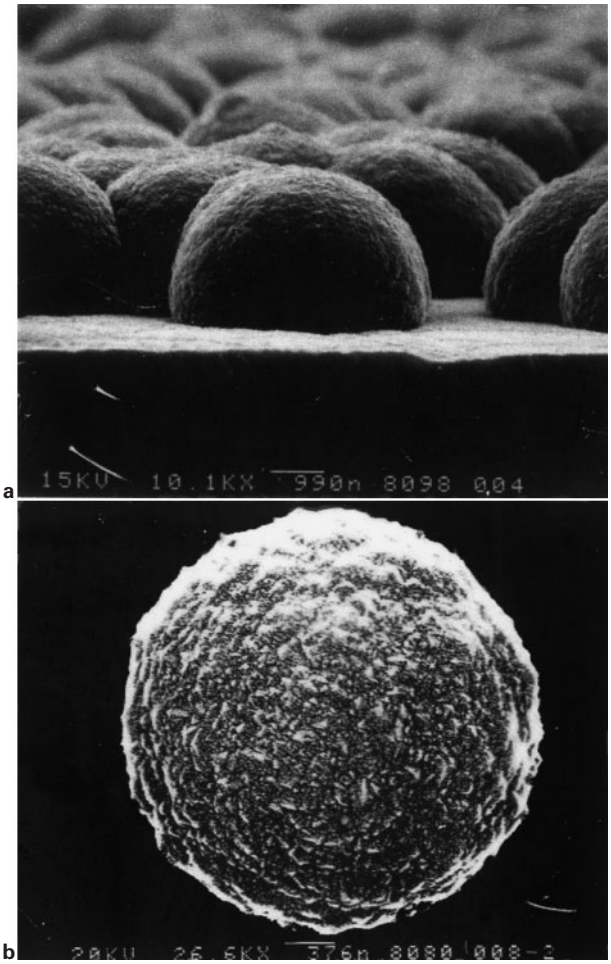

a profile, scale bar represents 990 nm; *b* plan view, scale bar represents 376 nm

1 Cauliflower structure of diamonds obtained under following CVD conditions: 4 h deposition time, 2273 K filament temperature, 1223 K substrate temperature, 10 torr reactor pressure, and $3CH_4$–$97H_2$ gas mixture (SEM)

three important experimental observations will be mentioned here.

1. CVD diamond forms relatively easily on a graphite surface.[49,50] In addition, almost all carbon allotropes are known to be beneficial to diamond initiation.[45] From the atomistic view of crystal growth, graphite should be the most unfavourable substrate for the growth of diamond, which should compete with graphite in nucleation and growth. While diamond has a nucleation barrier on a graphite substrate, graphite has no additional barrier for nucleation on a graphite substrate.

The poisonous effect of graphite for metastable growth of diamond is well established in the 'old' diamond CVD process not using gas activation.[48,51] Since the growth unit in the old CVD diamond process is an atom, it is worth a brief discussion. In the old process, a diamond seed was used as a substrate while a gas mixture of methane and hydrogen was decomposed thermally on the substrate. The impractically low growth rate of a few angstroms per hour in this process comes from the formation of graphite debris on the growing diamond surface.[48,51] This graphite debris is believed to form by gas phase nucleation. The formation of neutral gas phase nuclei sets an upper limit of the growth rate by atomic deposition. Once the graphite debris is formed, the entire diamond surface is covered with a graphitic layer, because of a much higher growth rate of graphite. For further growth, the graphite layer should be etched; the process needed cyclic etching.

Therefore, it is surprising that graphite is relatively favourable for diamond formation in the new process. This phenomenon is difficult to explain without assuming that diamond clusters form in the gas phase and land on the graphite substrate. Because of the additional carbon source provided by hydrogen etching the graphite substrate, clusters approaching a graphite substrate will be etched at a much lower rate than those approaching a non-carbon substrate. This would be why the graphite substrate is more favourable for diamond initiation.

2. The second experimental observation implying diamond growth by charged clusters is the cauliflower structure, as shown in SEM images (Fig. 1), which evolves when the methane concentration is high. In this structure, each macroparticle of a few micrometres consists of numerous tiny nodules of tens of nanometres. For the formation of the tiny nodules shown in Fig. 1 by the atomic unit, secondary nucleation should have taken place on the growing surface. Such a high frequency of secondary nucleation requires a gas phase with a much higher supersaturation of depositing species than for onset of diffusion controlled growth by kinetic roughening. Since there exists no barrier for atomic attachment on the kinetically roughened surface, the supersaturation for secondary nucleation does not build up on the growing surface and the surface undergoes just growth without secondary nucleation.

Therefore, a classical account in terms of atomic unit deposition is hardly successful to explain the observed growth of such a cauliflower structure. Since the evolution of a cauliflower structure is unique to thin film growth by charged clusters, the structure can be used as a microstructural criterion for such growth.[52]

3. When silicon and iron substrates are placed side by side, a dense diamond film deposits on the silicon substrate, while porous and skeletal soot deposits on the iron substrate. The soot is very fragile. Since the soot is easily smeared, the soot particles are weakly connected to each other by van der Waals forces. Atomic growth cannot explain this evolution of highly porous soot, which can be best explained by aggregation of particles formed in the gas phase. The growth mechanism of soot provides a critical clue to the development of the TCC[3] and will be explained in more detail in the section describing the effect of substrates on the deposition of charged clusters.

Experimental confirmation of charged clusters

Experimental confirmation of the existence of charged clusters is critical to the validity of the TCC. In order to confirm their existence in a hot filament diamond CVD process, the hypothetical clusters in the reactor were extracted into a high vacuum chamber by the standard method of orifice sampling using differential pumping.[16] Two-stage orifice sampling was used so that the system is divided into three chambers, as shown in Fig. 2. The first and the second orifices are concentric and have hole diameters of 1·2 and 2·0 mm, respectively.

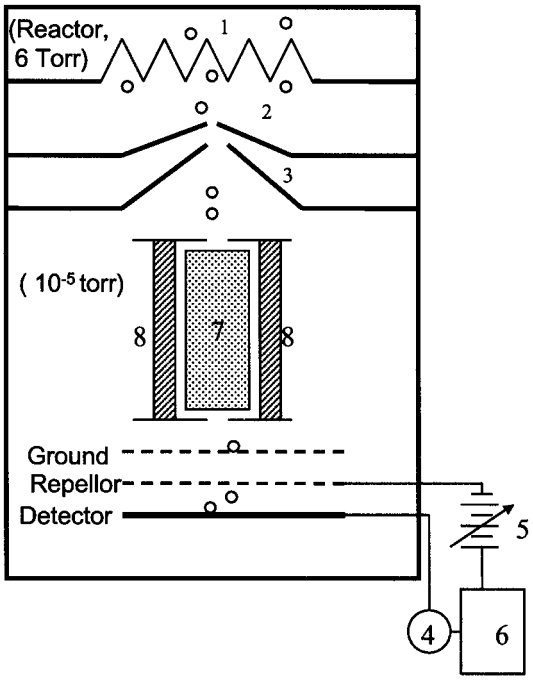

1: filament; 2: sampling orifice (1·2 mm dia.); 3: skimmer orifice (2·0 mm dia.); 4, 5: electrometer (Kethely 617); 6: computer; 7: electrodes; 8: magnets (7300 G)

2 Hot filament CVD system with Wien filter and energy analyser to determine mass distribution of hypothetical negatively charged carbon clusters generated during CVD diamond deposition (reprinted from Ref. 16, ©2000, with permission from Elsevier Science)

The extracted beam goes into a Wien filter, which allows charged clusters only with a specified velocity to pass through; charged clusters with other velocities are deflected to the walls of the filter. The velocity-selected charged clusters fly towards the current detector, which detects the amount of charged clusters as an electric current. A repelling potential mesh is placed just above the current detector. According to previous theoretical and experimental results on maximum electron charge and particle size in dry air,[53] particles smaller than $\sim$10 nm are singly charged. Since the clusters concerned here are far less than $\sim$10 nm, charged clusters would be singly charged.

If a repelling potential is applied, the negatively charged clusters with kinetic energy less than the repelling potential will be repelled and not detected on the current detector. Thus, with increasing repelling potential, the current on the detector decreases. Differentiation of the current with respect to the repelling voltage produces the energy distribution of charged clusters. Since the velocity and the energy ($1/2mv^2$) of clusters are known, their mass distribution can be determined. By adjusting the electric field of the Wien filter, clusters with other velocities can be selected and their mass distribution determined. Then, the accumulation of the mass distributions of clusters with different velocities produces the overall mass distribution of the charged clusters in the reactor.

In this way, the mass distribution of charged clusters in the hot filament diamond CVD reactor was determined under typical processing conditions: 6 torr reactor pressure, 1·5CH_4–98·5H_2 gas mixture, and

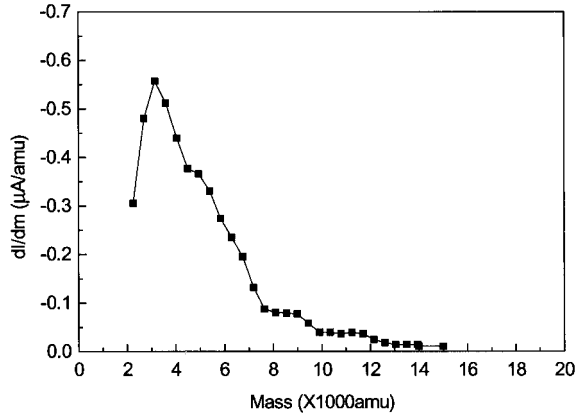

3 Mass distribution of negatively charged carbon clusters extracted from hot filament reactor: distribution shows peak at $\sim$3000 amu, which corresponds to clusters containing $\sim$250 carbon atoms (reprinted from Ref. 16, ©2000, with permission from Elsevier Science)

2373 K filament temperature (*see* Fig. 3).[16] The peak is at $\sim$3000 amu (atomic mass unit), which corresponds to $\sim$250 carbon atoms. It should be noted that most current is carried by the clusters rather than by atoms or molecules. Positive current was negligible and almost all clusters were negatively charged in the hot filament diamond CVD process.

Effect of methane concentration on cluster size

Experimentally, high quality diamonds with well defined facets are grown with a low methane concentration, while poor quality diamonds such as those of cauliflower-shaped structure are grown with a high methane concentration. According to the TCC, this effect of methane concentration was explained by the cluster size, which was suggested to increase with increasing methane concentration.[3] Furthermore, it was suggested that for a given substrate temperature, small clusters undergo epitaxial recrystallisation relatively easily, producing high quality diamonds, while large clusters frequently fail in epitaxial recrystallisation and tend to make twins or grain boundaries, producing poor quality diamonds with a cauliflower-shaped structure.

The effect of methane concentration on the cluster size was studied using a retarding potential analyser combined with the relationship between cluster size and velocity determined using a Wien filter.[17] The results are shown in Fig. 4. Most clusters for low methane concentration (1·0 and 1·5%CH_4) contain a few hundred carbon atoms. On the other hand, there exists an appreciable amount of large clusters containing more than 1000 carbon atoms for high methane concentration (3·0 and 5·0%CH_4).

During the energy distribution measurements, diamonds were deposited *in situ* on a molybdenum substrate placed near the sampling orifice, with a substrate temperature of 1023 K. The diamond films deposited at 1 and 1·5%CH_4 showed good crystalline quality, while those at 3 and 5%CH_4 showed a ball-like or cauliflower-shaped structure, as has been well established in the diamond CVD process.[45] Figures 5*a* and 5*b* show SEM images after deposition for 1 h at 1 and 3%CH_4, respectively.[17] These results agree with the TCC in that the cluster size increases with increasing

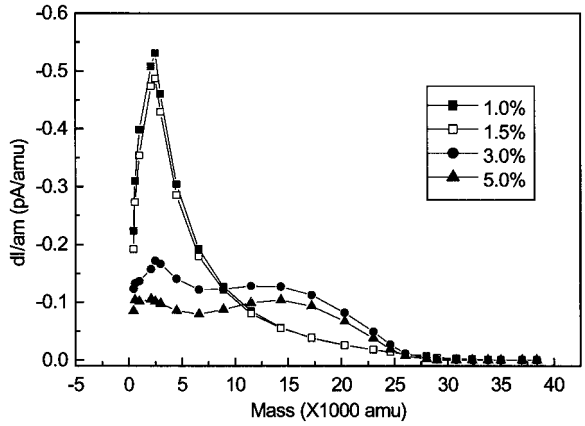

4 Mass distributions of negatively charged carbon clusters extracted from hot filament reactor using $1CH_4$–$99H_2$, $1{\cdot}5CH_4$–$98{\cdot}5H_2$, $3CH_4$–$97H_2$ and $5CH_4$–$95H_2$ gas mixtures, 2373 K filament temperature, and 6 torr reactor pressure: size of clusters tends to increase with increasing methane concentration (reprinted from Ref. 17, ©2001, with permission from Elsevier Science)

methane concentration and small clusters produce high quality diamonds with well defined facets, while large clusters produce poor quality diamonds with a ball-like or cauliflower-shaped structure.

Mass distribution of charged carbon clusters measured in oxyhydrocarbon flame by Homann group

Homann and co-workers[54–57] carried out extensive studies of mass distributions of charged clusters generated in the flame of an oxyhydrocarbon gas mixture using a Wien filter, an energy analyser, and time-of-flight mass spectroscopy (TOF-MS). Although their study was focused on the mechanism of soot formation in the flame of combustion, their results provide valuable information in regard to the TCC, especially in the diamond CVD process.

The carbon/oxygen ratio they used was close to one, where diamond can be deposited according to the Bachmann diamond deposition diagram.[58] Gerhardt and Homann[55] used several types of hydrocarbon–oxygen flames with a typical C/H/O ratio of $1{\cdot}02:1{\cdot}02:1$. They varied the carbon/oxygen ratio in order to control the flame of the burner to be oxidising or reducing. It should be noted that this composition can produce a diamond film according to previous results of acetylene flame experiments[59,60] or the Bachmann diagram for diamond deposition.[58]

Gerhardt and Homann[55] also determined the mass distributions of positively charged carbon clusters with varying distance from the burner of an acetylene–oxygen flame. For example, for gas sampling at a distance of 15 mm from the burner, the maximum current of the charged clusters, which was $\sim 1{\cdot}5$ pA, was measured at ~ 25000 amu, which corresponds to ~ 2000 carbon atoms. In a study using a butadiene (C_4H_6)–oxygen flame,[57] the maximum frequencies of positively charged clusters at gas sampling distances of 25, 30, 35 and 40 mm from the burner occurred at ~ 8000, ~ 14000, ~ 18000, and ~ 24000 amu, respectively. On the other hand, the mass distributions for negative carbon clusters were a little broader and weighted more towards larger masses. The maximum frequencies of the mass for the corresponding distances were ~ 10000, ~ 15000, ~ 19000, and ~ 25000 amu, respectively.

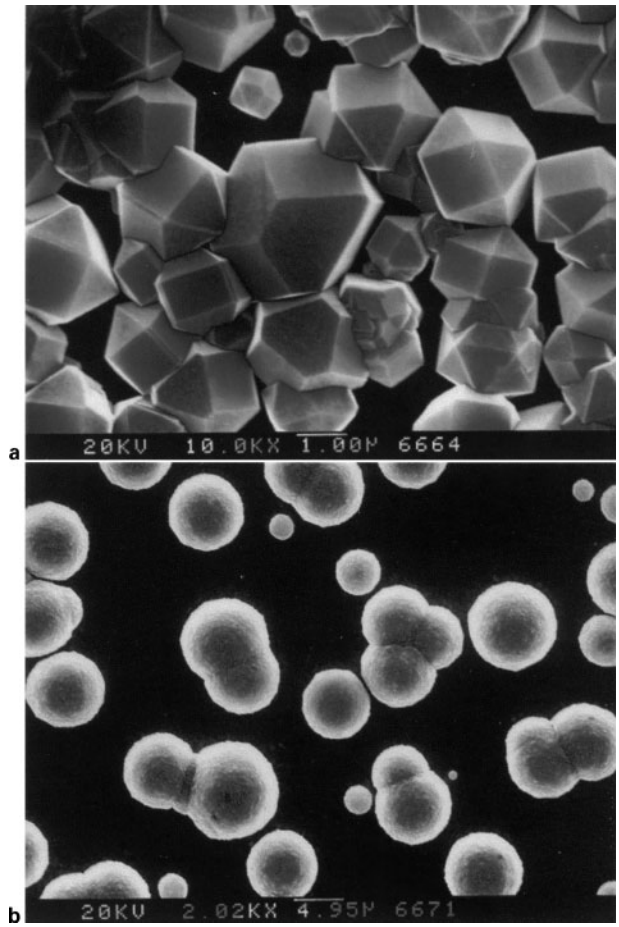

a **$1CH_4$–$99H_2$: clusters of narrow size distribution containing mainly just few hundred atoms produce high quality diamond crystals with well defined facets (scale bar represents 1 μm);** ***b*** **$3CH_4$–$97H_2$: clusters of broad size distribution containing up to more than 1000 atoms produce poor quality diamonds with cauliflower-shaped structure (scale bar represents 4·95 μm)**

5 SEM images of diamond films deposited *in situ* during measurement of mass distribution of charged clusters at 2373 K filament temperature and 6 torr reactor pressure (reprinted from Ref. 17, ©2001, with permission from Elsevier Science)

Gerhardt and co-workers[56,61] also used time-of-flight mass spectrometry (TOF-MS). Since the mass resolution by TOF-MS is high, they could determine the amount of hydrogen adsorbed. The positive clusters tended to have an appreciable amount of hydrogen, but the negative clusters did not. For an acetylene flame, the negative clusters were pure carbon, but for a benzene flame, the negative clusters contained one or two hydrogen atoms.[61] Gerhardt and Homann[56] identified the positive clusters as polycyclic aromatic hydrocarbon (PAH) ions.

Gerhardt and Homann[55] suggested that the PAH^+ ions, after growing to the size of $\sim 1{\cdot}5$ nm (~ 2000 amu), would undergo transition to pure carbon clusters, which they called soot. The negative clusters contained the fullerene (C_{60}). The mass distribution was centred on a pure carbon cluster containing about 100 carbon atoms. They believed the negative clusters in this mass range to have a cage structure and called them

polyhedral carbon. These clusters did not tend to grow even under conditions where the positive clusters grew appreciably.

The important result revealed through TOF measurements by the Homann group is that negatively charged clusters consist of almost pure carbon, while positively charged clusters are hydrogenated.[61] If this result is combined with the diamond deposition behaviour in the dc plasma process, where a diamond film grows on the anode and non-diamond carbon grows on the cathode, negatively charged carbon clusters, which are not hydrogenated, deposit as diamond films while positively charged clusters, which are hydrogenated, deposit as non-diamond carbon. This non-diamond carbon would deposit as an amorphous phase at substrate temperatures low enough for hydrogen not to be desorbed during deposition, while it would change to graphite at substrate temperatures high enough to desorb hydrogen. This analysis provides a new insight on the growth mechanism of amorphous films. To the present authors' understanding, amorphous silicon films are formed in a similar way; positively charged silicon clusters are hydrogenated and if deposited at a substrate temperature low enough for hydrogen not to be desorbed, they make amorphous silicon.[62] This problem will be treated in more detail below.

Observation of carbon clusters by TEM

In previous sections, negatively charged clusters of a few hundreds of carbon atoms were shown to exist in the diamond CVD process. These clusters can be observed if they are captured on a grid membrane for TEM. In order to capture the carbon clusters during the oxyacetylene diamond CVD process, a molybdenum mesh grid coated with an amorphous silica membrane for TEM was used. With a flowrate of 2 L min^{-1}, the flame length was 20 mm for a carbon/oxygen ratio of 1·04. Crystalline diamonds were deposited 16 mm away from the nozzle on a substrate placed on a water cooled copper plate. In order to capture the clusters under the diamond deposition condition, the molybdenum grid was placed 16 mm away from the nozzle on a water cooled copper plate.

Carbon clusters captured for 60 s with a carbon/oxygen ratio of 1·04 in an oxyacetylene flame are shown in Fig. 6.[18] Individual clusters are shown as dark spots. Isolated clusters with an average size of 1–1·5 nm are distributed uniformly on the amorphous silica membrane. The number density of clusters was $2{\cdot}0 \times 10^{11}$ mm^{-2}. In the high resolution TEM of Fig. 6*b*, most clusters did not show a lattice fringe, but some clusters show a lattice fringe spacing consistent with the (111) planes of a diamond structure, as circled in the figure.

The clusters in Fig. 6 are in the size range 1·0–1·5 nm and would contain a few hundreds of carbon atoms, which is comparable to the size distribution of negatively charged clusters measured in Figs. 3 and 4. The authors have not determined whether or not the negatively charged clusters in Figs. 3 and 4 have a diamond structure. However, Fig. 6*b* shows that at least some of them do. The fact that most clusters in Fig. 6*b* did not show a lattice fringe structure does not necessarily mean that the clusters do not have a diamond structure in the gas phase. Even if the clusters have a crystalline

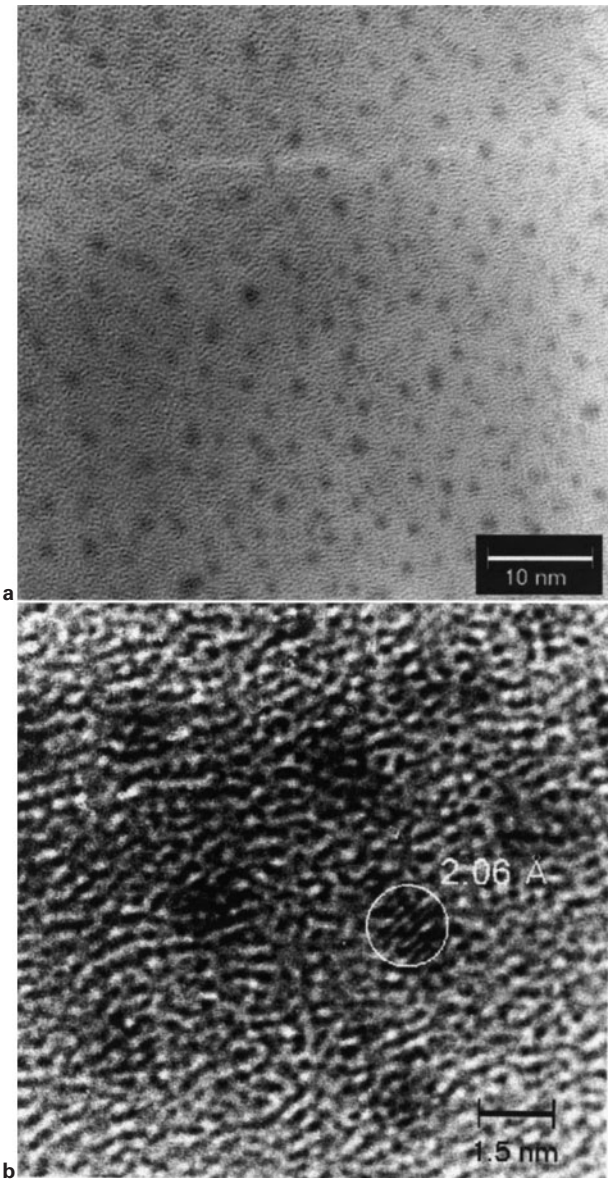

a scale bar represents 10 nm; *b* scale bar represents 1·5 nm

6 Carbon clusters captured on silica membrane for 60 s with C_2H_2/O_2 gas ratio of 1·04 : 1 during flame deposition of diamond (TEM): some clusters, as shown circled in *b*, show (111) lattice fringe of diamond (reprinted from Ref. 18, ©2002, with permission from Elsevier Science)

diamond structure in the gas phase, they can change to an amorphous structure on the amorphous silica membrane of the TEM grid. According to the authors' molecular dynamics simulation of the cluster deposition behaviour, even crystalline diamond clusters of a few nanometres can change instantaneously to an amorphous structure after depositing on the amorphous substrate. Another possibility is that crystalline clusters can appear amorphous depending on their orientation in the TEM observation.

Silicon CVD

Background

Because of its high Debye temperature, diamond is the material least expected to be able to grow by the

scale bar represents 1 μm

7 SEM image of cauliflower structure of silicon deposited for 10 min with $1SiH_4$–$1HCl$–$98H_2$ gas mixture, 1123 K substrate temperature, and 100 torr reactor pressure (reprinted from Ref. 52, ©2000, with permission from Hanyang University Press)

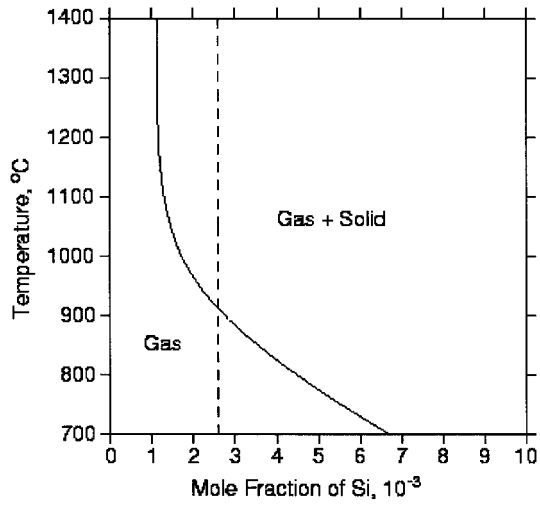

8 Temperature dependence of solubility of silicon (solid line) in gas phase in Si–Cl–H system (vertical dashed line represents composition used in process): thermodynamic calculation was carried out under conditions of 150 torr pressure and with 2·86 mol Cl and 201·06 mol H (reprinted from Ref. 19, ©1999, with permission from Elsevier Science)

building block of charged clusters. Since perfect diamond crystals can be grown by charged clusters containing hundreds of atoms, other materials are also expected to be able to grow by charged clusters. As the first step to study the generality of thin film growth by charged clusters, silicon CVD was chosen for detailed study because it is one of the most important systems in microelectronics. Based on microstructural analysis, there are at least three experimental indications that silicon film should grow by charged clusters.

1. The evolution of a cauliflower shaped structure (*see* Fig. 7) having the same microstructural characteristics as the diamond cauliflower structure shown in Fig. 1, which was evolved by the deposition of large clusters.

2. The evolution of a porous skeletal soot-like silicon structure on a substrate with a high charge transfer rate,[22] a phenomenon that is similar to the evolution of soot on an iron substrate in the diamond CVD process.[3] On a substrate with a low charge transfer rate, a dense silicon film with large grains with well developed facets tends to be evolved. This effect will be explained below in more detail.

3. The puzzling phenomenon of simultaneous deposition and etching of silicon reported by Kumomi and coworkers[63–65] in their selective nucleation-based epitaxy (SENTAXY) process, where silicon deposits selectively on periodic SiN_x patterns on SiO_2. In the initial stage (480 s) of their experiment, multiple fine particles were selectively formed on all SiN_x patterns. However, in the intermediate stage (720 s), one large cluster, which was apparently distinguishable, emerged among the pre-existing fine clusters on some of the SiN_x portions, while other particles disappeared due to etching. In the final stage (960 s), almost the entire area of each pattern was covered with one large particle while a few SiN_x patterns were vacant, where all particles on these patterns had been etched away. After analysing this phenomenon, the authors[63–65] concluded that it could not be explained by a coarsening process such as Ostwald ripening.

This phenomenon is similar to diamond deposition with simultaneous graphite etching in the diamond CVD process. Since the driving force, which is the chemical potential difference between silicon as a solid and a gas adjacent to the growing surface, is either for deposition or for etching, but cannot be for both, these two irreversible processes cannot take place simultaneously if the deposition unit is an atom. Simultaneous deposition and etching can be explained on a sound thermodynamic basis if gas phase nuclei are the building blocks of silicon films.

As in the case of the C–H system for diamond CVD, the solubility of silicon in the gas phase of the Si–Cl–H system increases with decreasing temperature near the substrate temperature, as shown in Fig. 8.[19] For example, the solubility of silicon in the gas phase is 0·00129 at 1100°C. The solubility increases to 0·00213 at a substrate temperature of 950°C. If silicon nucleates in the gas phase, the driving force at the substrate temperature changes to be for etching, because of the depletion of silicon in the gas phase. Under this situation, the silicon on the substrate will be etched away into the gas phase with simultaneous deposition onto the substrate of silicon clusters from the gas phase, which leads to the macroscopic observation of simultaneous deposition and etching of silicon.

Observation of silicon clusters by TEM

Since charged silicon clusters were predicted by the microstructural features described above, it was expected that silicon clusters could be observed by TEM, if they were captured on a copper grid with an amorphous membrane. However, it was difficult to capture them using thermal CVD, presumably because of the electrostatic repulsion between the membrane and the charged silicon clusters. By using hot tungsten filament CVD, the clusters were captured.[21] During the process, the negative current was measured to be 0·2–5 μA cm^{-2} on the substrate. The magnitude of negative current was about 5 times higher at the filament temperature of 2073 K than at 1873 K.

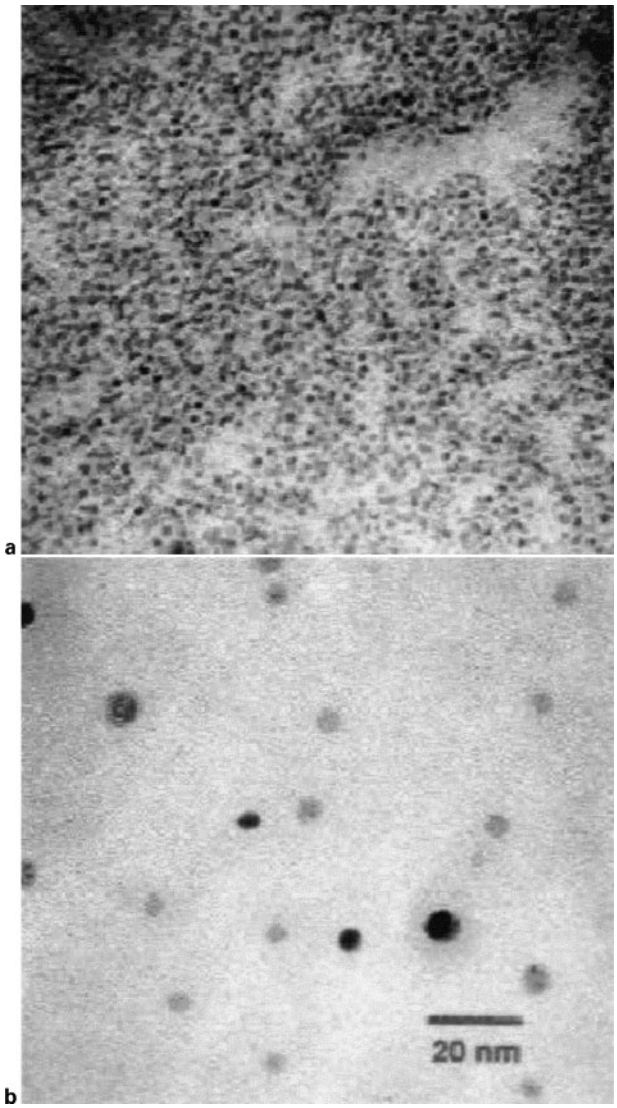

9 TEM images of silicon clusters captured on carbon membrane for $5SiH_4$–$1HCl$–$94H_2$ gas mixture at chamber pressure of 10 torr and substrate temperatures of *a* 2073 K and *b* 1873 K (reprinted from Ref. 21, ©1999, with permission from Elsevier Science)

Figure 9 shows TEM images of the nanosize clusters on a carbon membrane for the gas mixture $5SiH_4$–$1HCl$–$94H_2$ under a chamber pressure of 10 torr. Clusters prepared at 2073 K were $\sim$2 nm (Fig. 9*a*) and those at 1873 K were 5–7 nm (Fig. 9*b*). The smaller cluster size at 2073 K is related to the higher current. It is the present authors' general observation that the higher the detected current in the thin film reactor, the smaller the cluster size. For example, the current decreases markedly when a halogen lamp instead of a hot tungsten filament is used as a heating source. In that case, the cluster size was as large as $\sim$50 nm under the same processing conditions.[21]

Zirconia CVD

Generation of charged clusters can be easily checked by current measurement in a thin film reactor. The reason why clusters are charged so easily in a CVD reactor is related to the fact that clusters have an intermediate property between a single atom and bulk. The ionisation potential of the cluster decreases with increasing cluster size, approaching a bulk work function value. Since the ionisation energy of clusters is much lower than that of a single atom or molecule, clusters are easily charged by surface ionisation under a normal thin film process, where a single atom or molecule is rarely charged.

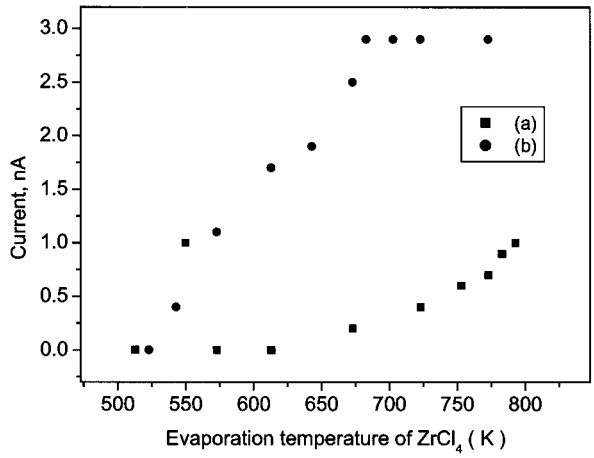

10 Current spontaneously produced (■) near evaporation temperature of $ZrCl_4$ and (●) at location for film deposition during ZrO_2 CVD (reprinted from Ref. 24, ©2001, with permission from Korean Ceramic Society)

The current measured during zirconia CVD is shown in Fig. 10, where the current is measured with the evaporation temperature of the $ZrCl_4$ precursor.[24] Here, the current was measured at two locations: near the precursor and at the substrate. The temperature near the precursor was about 100 K higher than the precursor temperature. The substrate temperature was fixed at 1273 K. The current tended to increase relatively steeply in the temperature range 573–673 K and nearly saturated at 723–823 K. The collecting area for current was $\sim$50 mm^2 so that the current density is a few nA/cm^2.

In order to capture individual zirconia nuclei from the gas phase, a nickel grid with a silica membrane for TEM was attached to a liquid-nitrogen cooled stainless steel cold finger and exposed near the substrate at 1273 K for 60 s at the $ZrCl_4$ evaporation temperature of 523 K. The zirconia clusters observed by TEM are shown in Fig. 11. The cluster size was in the range 10–15 nm. The high resolution image of Fig. 11*b* shows the lattice fringe of a tetragonal zirconia structure.

Thermal evaporation of metals

Effect of bias on deposition behaviour

Compared to the CVD process, the thermal evaporation process is carried out in relatively high vacuum. Because of the long mean free path, atomic collision for clustering in the gas phase is much less frequent than in the CVD process. Although thin film processes by sputtering and laser ablation are carried out in relatively high vacuum, generation of charged or neutral clusters as well as charged and neutral atoms is well established.[66–68] In these high vacuum processes, clusters are not formed in the gas phase, but are emitted from the target. In the thermal evaporation process, the base pressure is normally less than 10^{-6} torr, although the pressure increases to 10^{-3}–10^{-4} torr during the evaporation process. Experimentally, it has been confirmed that

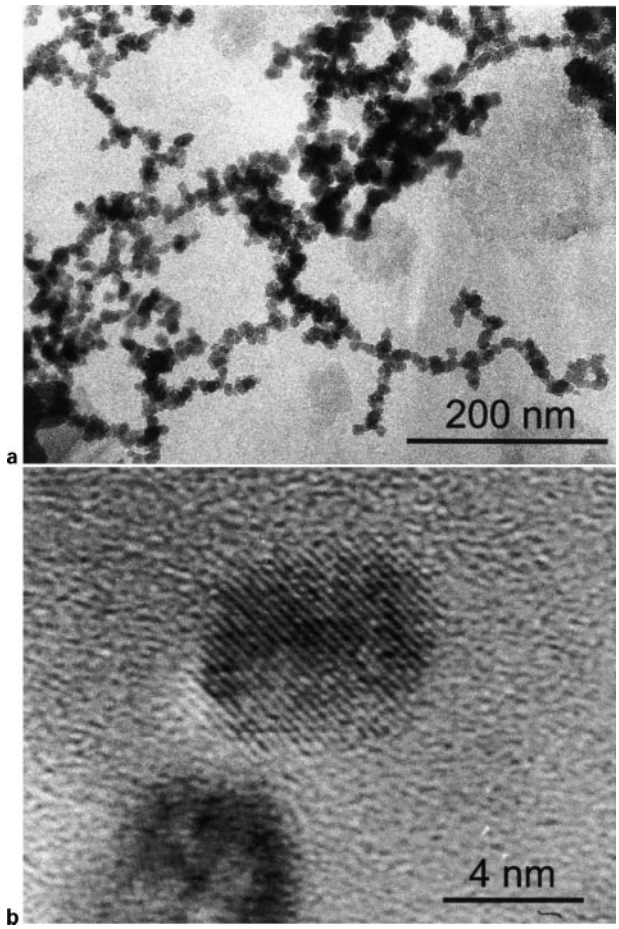

11 ***a*** **Low and** ***b*** **high magnification TEM images of zirconia clusters captured, for 60 s at $ZrCl_4$ evaporation temperature of 523 K, on grid membrane attached to cold finger and exposed near substrate (reprinted from Ref. 24, ©2001, with permission from Korean Ceramic Society)**

charged or neutral clusters are generated during thermal evaporation of metals.[11,25,69] It appears that those clusters are formed in the gas phase instead of being emitted directly from evaporating metals.

Owing to the relatively long mean free path in the reactor, charged clusters, once formed, will be attracted or repelled by an applied electric bias. Therefore, if a bias is applied during thermal evaporation of metals, the deposition behaviour will clearly reveal whether charged clusters are generated or not. Figure 12 shows TEM images of clusters captured on an amorphous silica membrane after 10 s of copper evaporation at 1573 K under applied bias voltages of $+200$, 0, and -200 V between a stainless block supporting the membrane and the chamber.[69] When a positive bias was applied (Fig. 12*a*), clusters were rarely observed. In the zero bias case (Fig. 12*b*), small clusters of approximately 2–4 nm were observed on the grid with a number density of approximately $4{\cdot}5\times10^{10}$ mm^{-2}. Clusters deposited under a negative bias (Fig. 12*c*) were larger (6 ± 2 nm), but appeared to be slightly less numerous ($9{\cdot}3\times10^{9}$ mm^{-2}).

Cross-section SEM images of copper films deposited on a (001) silicon wafer under applied bias voltages of $+400$, 0, and -400 V, respectively, are shown in Fig. 13. Again, a clear bias effect can be seen. The $+400$ V bias

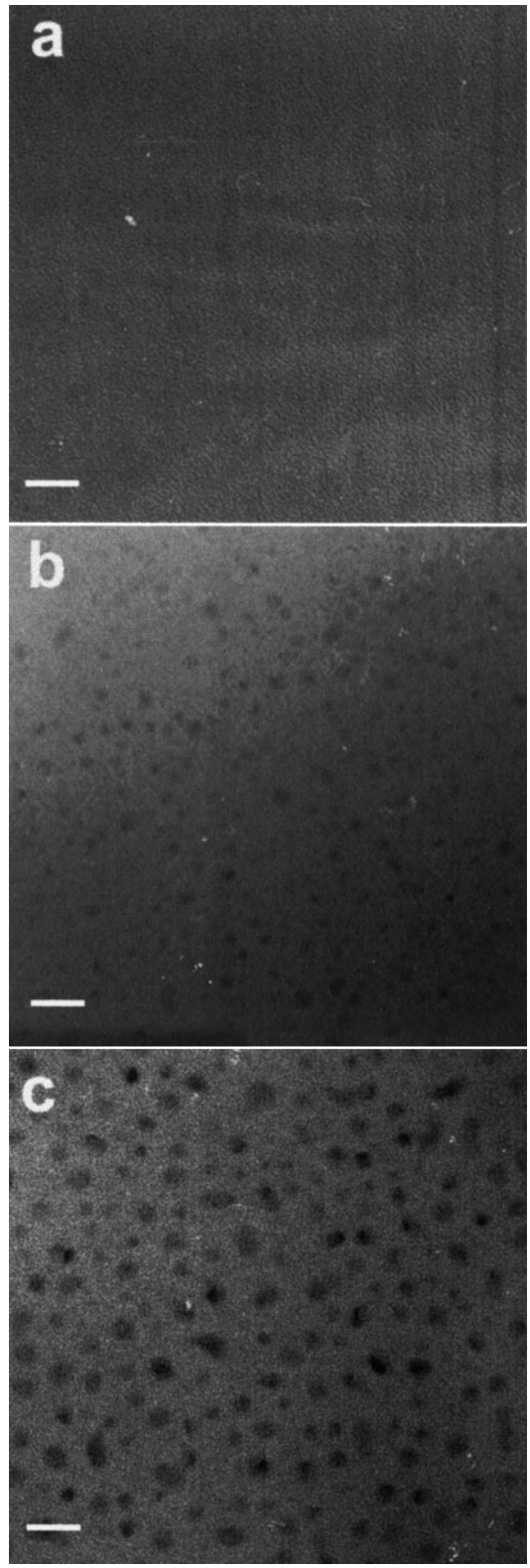

12 Clusters deposited on silica membrane under electric bias of ***a*** **$+200$,** ***b*** **0, and** ***c*** **-200 V for 10 s of copper evaporation at 1573 K (scale bar in each TEM image represents 10 nm): negligible deposition on substrate biased $+200$ V implies that main deposition flux is positively charged (reprinted from Ref. 26, ©2002, with permission from Elsevier Science)**

sample (Fig. 13*a*) shows a film of ~10 nm thickness in comparison with films of ~100 nm for zero bias (Fig. 13*b*) and ~120 nm for -400 V bias (Fig. 13*c*).

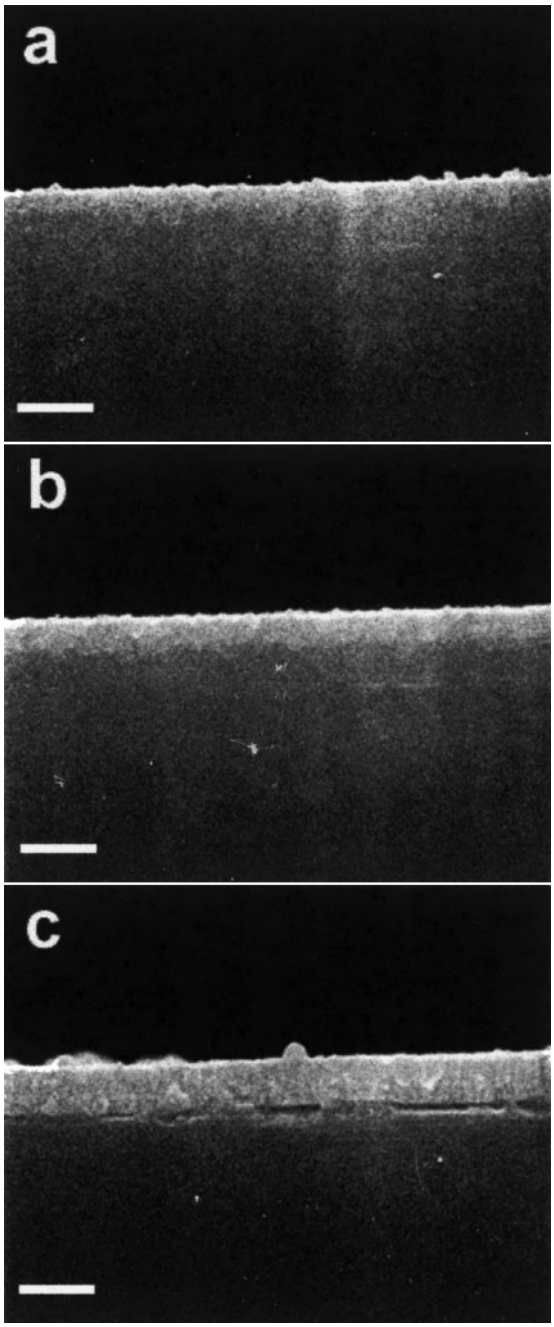

13 Copper films deposited on silicon wafer under electric bias of *a* +400, *b* 0, and *c* −400 V for 5 min of copper evaporation at 1573 K (scale bar in each SEM image represents 100 nm): relatively much smaller film thickness on substrate biased +400 V implies that main deposition flux is positively charged (reprinted from Ref. 26, ©2002, with permission from Elsevier Science)

This means that a positive bias repels most of the copper from the silicon substrate and suggests that there may be a small flux of neutral atomic or cluster deposition. The fact that clusters were hardly observed in Fig. 12*a* does not mean that they were not present as they may have been too small to be observed by TEM. In the negative film of TEM, clusters less than ~0·5 nm could be vaguely, but reproducibly, observed. These clusters would contain about 20 atoms and could not be resolved in the positive photograph. These clusters appear to be formed by atomic unit deposition on the substrate.

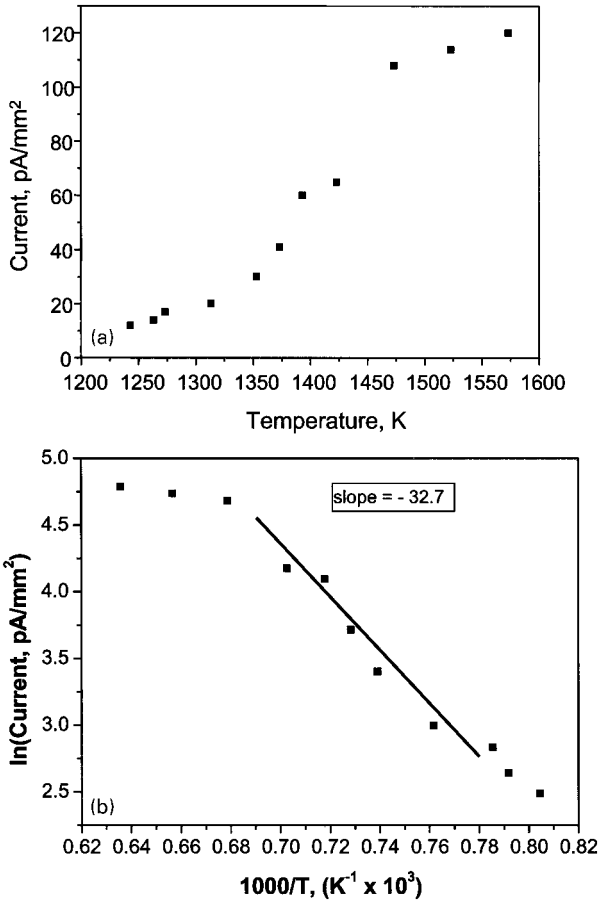

14 *a* Temperature dependence of electric current detected on Faraday cup during copper evaporation and *b* plot of logarithm of current against inverse of absolute temperature (reprinted from Ref. 12, ©2003, with permission from Elsevier Science)

From Fig. 13, the increased thickness observed in the negative bias case can be explained by considering that most clusters were positively charged. In the zero bias case, copper deposition can occur anywhere in the chamber, whereas in the negative bias case, copper is attracted to the substrate surface. This result is in qualitative agreement with Fig. 12*c* where the greatest amount of overall deposition was also observed when an attractive bias was applied.

Origin of electric charging during thermal evaporation

Understanding the charging mechanism of clusters is crucial to understanding the growth mechanism of thin films. In particular, the percentage of charged copper clusters at 1573 K was reported to be unusually high.[69] Figure 14*a* shows the dependence of the current on the evaporation temperature.[12] Current was not detected below 1240 K, began to appear above 1240 K, and thereafter increased with increasing evaporation temperature. The current increased steeply above the melting point of copper (1356 K) and then increased only slightly above 1473 K. Considering the ionisation potential of copper (7·7 eV),[70] the amount of current generated during evaporation of copper at 1573 K is surprising. The mechanism of positive charging can be analysed by evaluating the activation energy from the temperature dependence of the current in Fig. 14*a*.

Figure 14*b* shows a plot of the natural logarithm of the current against the inverse of the evaporation temperature. The plot shows two different slopes, which were determined by least squares fitting. Below and above 1473 K, the slopes were –32·7 and –2·4, respectively, with the respective activation energies of 2·81 and 0·2 eV. The slope change in Fig. 14*b* arises from the generation of negative current, which was detected above 1348 K and increased with increasing temperature. Therefore, 2·81 eV is a reasonable estimation for the activation energy of positive charging.

It is known that the ionisation potential of an atom or molecule decreases drastically when the atom evaporates from or collides with a surface and thereby loses an electron not in a vacuum but in a surface.[6,8] This phenomenon is known as surface ionisation and expressed by the Saha–Langmuir equation as follows[8]

$$\frac{n^+}{n^0} = \frac{g^+}{g^0} \exp\left(-\frac{\phi - W}{kT}\right) \tag{1}$$

where n^0 and n^+ are the number densities of a neutral atom and its ion, respectively, g^0 and g^+ are the statistical weights of the neutral atom and its ion, respectively, ϕ is the ionisation potential of the atom, k is Boltzmann's constant, and W and T are the work function and the temperature of the ionisation filament surface, respectively. The term n^0 corresponds to the equilibrium vapour pressure of copper, which is given as

$$n^0 \propto \exp\left(-\frac{\Delta H_{\text{evap}}}{kT}\right) \tag{2}$$

where ΔH_{evap} is the heat of evaporation of copper.

If equation (2) is substituted in equation (1), the number density of positive copper ions is given by

$$n^+ \propto \exp\left(-\frac{\Delta H_{\text{evap}} + \phi - W}{kT}\right) \tag{3}$$

If the current detected during copper evaporation as shown in Fig. 14*a* is due to the surface ionisation of a copper atom, the activation energy for positive charging should be given by equation (3) as $\Delta H_{\text{evap}} + \phi - W$.

From vapour pressure data,[70] ΔH_{evap} is estimated to be 3·26 eV. Therefore, $\phi - W = -0{\cdot}45$, which indicates that positive charging is a spontaneous process. The ionisation potential ϕ of copper is 7·7 eV.[70] The surface for surface ionisation during evaporation of copper in a tungsten basket can be copper, tungsten, or tungsten oxide. The work functions of copper, tungsten, and tungsten oxide are 4·7, 4·5, and 6·2 eV, respectively.[70] The values for $\phi - W$ for the work functions of copper, tungsten, and tungsten oxide are 3·0, 3·2, and 1·5 eV, respectively. These values are much higher than $-0{\cdot}45$ eV, which is determined from the measured current in Fig. 14.

If clusters are formed in the gas phase during evaporation, their ionisation potential is much lower than that of a single atom. The ionisation potentials of copper clusters Cu_n with n=15–41 were reported to be in the range 5·1–5·9 eV.[71]

For positive charging of copper clusters, the Saha–Langmuir equation (1) can be rewritten as

$$\frac{n^+_{\text{cluster}}}{n^0_{\text{cluster}}} \propto \exp\left(-\frac{\phi_{\text{cluster}} - W}{kT}\right) \tag{4}$$

where the parameters with the subscript represent the values for a cluster. If 5·1 eV for ϕ_{cluster} and 6·2 eV for the work function of tungsten oxide are substituted, the value is $-1{\cdot}1$ eV. If 5·9 eV for ϕ_{cluster} and 6·2 eV for the work function of tungsten oxide are substituted, the value is $-0{\cdot}3$ eV. The value of $-0{\cdot}45$ eV falls in this range. Therefore, the surface ionisation of clusters on the tungsten oxide can best explain the origin of the low temperature positive charging of a copper source generated during thermal evaporation of copper.

Since the work function of tungsten oxide is relatively large and therefore favourable for surface ionisation, the possibility for oxidation of a tungsten basket during thermal evaporation will be mentioned briefly. The minimum oxygen partial pressure for oxidation of tungsten at 1573 K is $\sim 4 \times 10^{-8}$ torr. Thus, the tungsten basket is expected to oxidise at least slightly under a vacuum of $\sim 5 \times 10^{-6}$ torr by a diffusion pump, while it would not in an UHV (ultrahigh vacuum) chamber. The degree of oxidation will depend on the processing conditions. In the present authors' experience, a poor vacuum is much more favourable for generating positively charged clusters during metal evaporation than a high vacuum, which implies that positive charging by surface ionisation is favoured by the high work function of tungsten oxide.

No current higher than the noise level of ~ 10 pA mm^{-2} was detected at an evaporation temperature of 1223 K, while more than 100 pA mm^{-2} was detected at 1573 K (Fig. 14). From this current measurement, the clusters generated at 1573 K are expected to be mostly positively charged, but it is not clear whether those at 1223 K, if any, are charged or neutral. The deposition behaviour at the evaporation temperatures of 1223 and 1573 K was compared and the results are shown in Figs. 15 and 16, respectively.[12] The film growth rate for 1223 K ($\sim 0{\cdot}01$ nm s^{-1}) was about 300 times lower than that for 1573 K (~ 3 nm s^{-1}). Therefore, the deposition time for Fig. 15 was set to 140 min and that for Fig. 16 was set to 7 min.

Although the growth rate was extremely low at the evaporation temperature 1223 K, the film morphology was much worse than that evaporated at 1573 K. Since the surface roughness shown in Fig. 15 was not expected to result entirely from atomic deposition, some neutral clusters appeared to have been generated during evaporation at 1223 K. It is known that the soft landing of small neutral clusters results in the random aggregation characteristic of a fractal structure when surface diffusion is not appreciable.[72] The reason why these clusters were not charged would be the small size with a relatively high ionisation potential, which prevented the clusters from undergoing surface ionisation. The smooth morphology of the film evaporated at 1573 K shown in Fig. 16 is attributed to deposition by a major flux of charged clusters. These results imply that a high deposition flux of charged clusters might produce denser and smoother films than a low deposition flux of neutral clusters.

Mechanism of cluster charging in the thin film process

In the case of sputtering[66,67] and laser ablation,[68] emission of neutral or charged clusters from the target is well established. If the reactor is in high vacuum with long mean free path, further collisions between clusters will not be appreciable and most neutral clusters remain

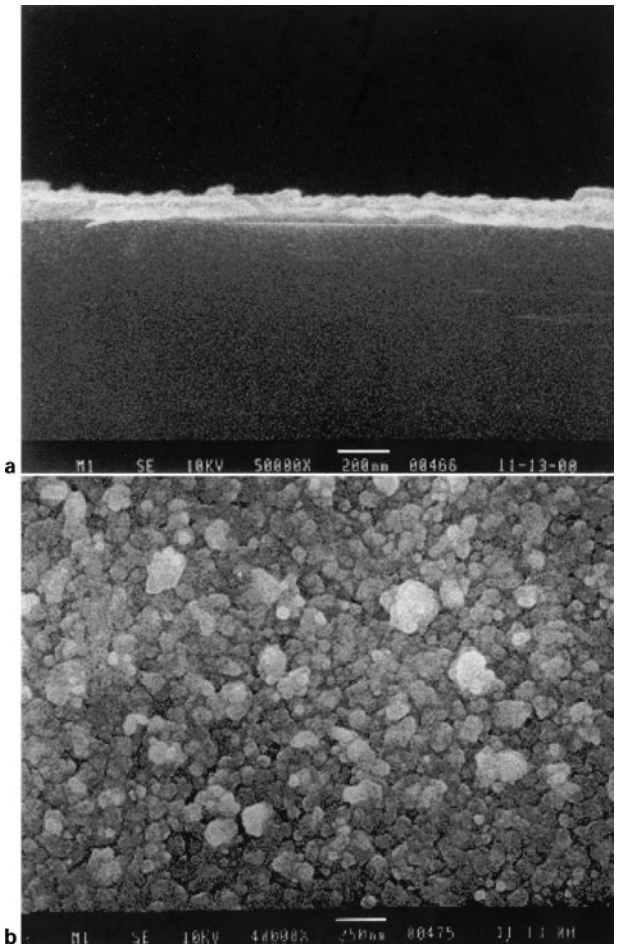

a cross-section, scale bar represents 200 nm; *b* plan view, scale bar represents 250 nm

15 Field emission SEM images of morphology of films deposited by evaporation of copper at 1223 K for 140 min (reprinted from Ref. 12, ©2003, with permis sion from Elsevier Science)

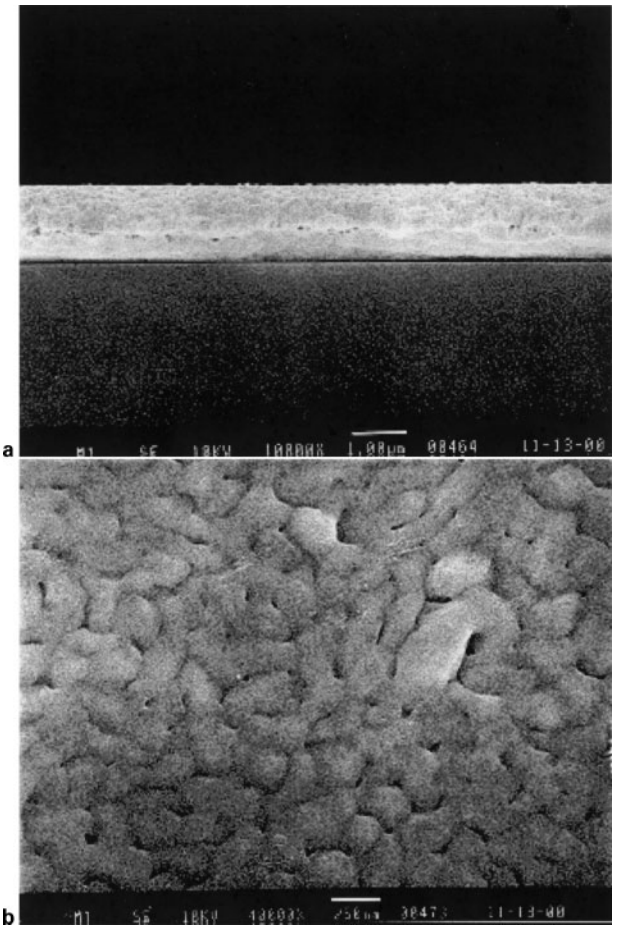

a cross-section, scale bar represents 1080 nm; *b* plan view, scale bar represents 250 nm

16 Field emission SEM images of morphology of films deposited by evaporation of copper at 1573 K for 7 min: in spite of film growth rate 300 times higher than that of Fig. 15, film surface is much smoother (reprinted from Ref. 12, ©2003, with permission from Elsevier Science)

neutral. As shown in the previous section, neutral clusters would produce poor quality films with voids, visible as a surface haze. If the reactor is in moderate vacuum with short mean free path, neutral clusters may become charged after collision with charged clusters or atoms. The number density of neutral clusters will decrease, resulting in deposition of better quality films. In this sense, a moderate vacuum is beneficial to promote charging of the clusters, which is beneficial again in producing void-free films. Physical vapour deposition is performed in relatively high vacuum, while CVD is performed in moderate vacuum. Therefore, CVD is more beneficial than PVD in charging clusters. This is why CVD tends to produce films with better quality and fewer voids than PVD.

In the non-plasma CVD process, surface ionisation appears to be the main charging mechanism. According to the Saha–Langmuir equation,[8] a heated surface with high work function is favourable for positive surface ionisation, while a heated surface with low work function is favourable for negative surface ionisation. Atoms, molecules, or clusters with low ionisation potential are favourable for positive surface ionisation, while those with high electron affinity are favourable for negative surface ionisation.

Deposition behaviour of charged clusters

Selective deposition

In the thin film process, it is frequently observed that deposition is more favourable on a conducting substrate than on an insulating substrate. Based on this, the technique of selective deposition has been extensively used in microelectronics.[63,73–76] In spite of the technological importance of this phenomenon, its underlying principle is not yet clearly understood. Selective deposition can be best understood by considering that charged clusters are the major deposition flux for growth of thin films.

Charged clusters will easily land on conductors, but have difficulty in landing on insulators, especially when the gas phase is insulating.[20] Coulomb repulsion between charged clusters and an insulating surface depends on the cluster size as well as on the conductivity of the clusters. Since the electric charge moves freely in the conducting cluster, the charge will move backwards in the cluster when the charged cluster approaches the insulating surface charged with the same sign. This backwards movement of charge, which will increase with

increasing cluster size, will diminish the Coulomb repulsion and sometimes reverse it into Coulomb attraction. Therefore, small clusters are favourable for selective deposition. Besides, conducting materials would have much more difficulty in selective deposition than semiconducting or insulating materials. When the gas phase is made conducting by a plasma, the selective deposition changes to non-selective deposition.[73,77] Since neutral clusters have no selectivity, their formation should be avoided for selective deposition. Neutral clusters can be avoided if the reactor pressure is so high that charged and neutral clusters collide frequently enough. Since MBE (molecular beam epitaxy), sputtering, and laser ablation are operated in high vacuum, they are not suitable for selective deposition.

Although charged clusters are thought to be a major depositing flux in the CVD process, deposition by an atomic flux is a kinetically parallel process, also contributing to film growth. Since atoms are neutral, atomic deposition is not selective, and thus would be expected to be detrimental to selective deposition. When clusters are formed in the gas phase, however, the total surface area of the clusters is so large that clusters capture most of the supersaturated atoms in the gas phase and the driving force for further precipitation at the substrate is usually small. If this driving force is so small as not to overcome the nucleation barrier on the substrate, the atomic flux is negligible and should not be detrimental to selective deposition.

In some systems, such as C–H (Ref. 13) and Si–Cl–H (Ref. 19), the gas phase solubility of depositing species is retrograde around the substrate temperature. As mentioned above, the gas phase nucleation in these systems would make the driving force at the substrate for etching. In this case, the atomic flux contributes negatively to film growth because etching takes place. Even if the deposition is non-selective in the initial stage where the charge built up on the substrate is small, the particles on the insulating area of the substrate can be etched away eventually.[20] Therefore, selective deposition can be ideally controlled. As will be explained in detail below, one-dimensional growth of nanotubes or nanowires is related to selective deposition of charged clusters on the tip rather than on the side of the wire.

Effect of substrates

In electrochemistry, the rate determining step is the rate of hydrogen evolution at the electrode, where electrons and hydrogen ions combine to evolve hydrogen gas. In order of decreasing rate of hydrogen evolution or charge transfer rate (CTR), the electrode materials are Pd, Pt, Rh, Ir, Ni, Fe, Au, W, Ag, Nb, Mo, Cu, Ta, Bi, Al, and Ti.[78] It was found that the substrate materials making soot in the diamond CVD process correspond to materials having a high CTR. The correlation between diamond or soot formation and CTR was very high: Pd,[79] Pt,[79,80] Rh,[79] Ir,[79] Ni,[80,81] Fe[81] are the substrate materials making soot or a non-diamond phase, while Au, W, Ag, Nb, Mo, Cu, Ta, [42,79,82,83] Al,[84] and Ti[85] are the substrate materials making diamond. Bismuth has too low a melting point to be used as a substrate.

Figure 17 shows the effect of the CTR of substrates in diamond CVD. Crystalline diamond particles are evolved on the silicon substrate with a low CTR (Fig. 17*a*), while porous skeletal graphitic soot is evolved

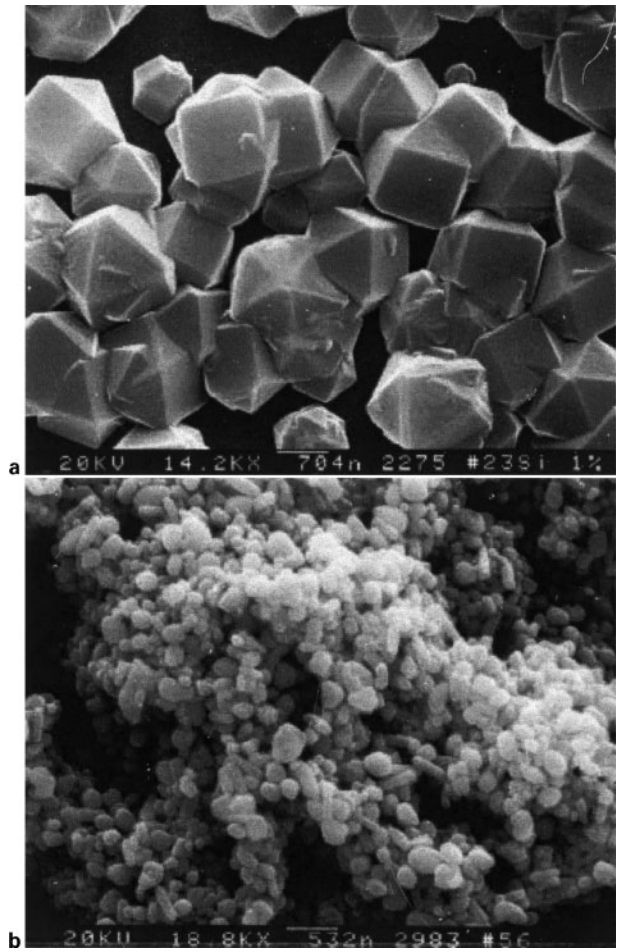

a scale bar represents 704 nm; *b* scale bar represents 532 nm

17 *a* Diamond deposited on silicon substrate and *b* soot deposited on iron substrate with $1CH_4$–$99H_2$ gas mixture for 2 h at substrate temperature of 1263 K under 20 torr (SEM): substrates were placed side by side during hot filament diamond CVD (reprinted from Ref. 3, ©1996, with permission from Elsevier Science)

on the iron substrate with a high CTR (Fig. 17*b*).[3] Although the diamond crystals in Fig. 17*a* do not give any hint as to whether they grew by atoms or clusters, the porous skeletal soot in Fig. 17*b* provides a critical hint as to its growth mechanism because of its peculiar morphology. The characteristics of soot in Fig. 17*b* are similar to those of soot commonly observed in the field of combustion and flame, where the mechanism of its formation has been intensively studied.[54–56,86] In this field, the primary soot particles are nucleated in the gas phase and tend to be electrically charged. The microstructure of Fig. 17*b* is difficult to explain by atomic unit deposition, because neither the growth by two-dimensional nucleation nor by ledge-generating sources such as screw dislocation can produce such a porous compact of soot. Furthermore, the soot in Fig. 17*b* is very fragile and is weakly connected between the particles; it can be easily smeared. Such weak bonding between particles implies that the growth unit is of small particles rather than of the atom. The morphology shown in Fig. 17*b* resembles the powder compacts formed by landing of particles, which are nucleated in the gas phase in the conventional CVD process.

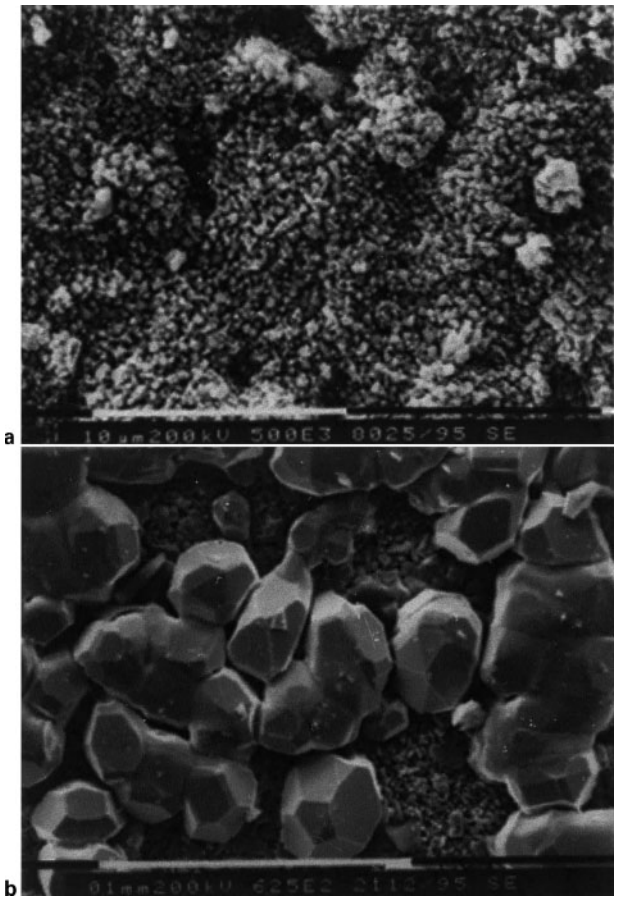

a scale bar represents 10 μm; *b* scale bar represents 100 μm

18 Silicon deposits after *a* 3 and *b* 30 min on nickel substrate with $1SiH_4$–1HCl–$98H_2$ gas mixture under reactor pressure of 10 torr at substrate temperature of 1123 K (SEM): porous skeletal structure like soot is evolved after 3 min on nickel substrate, which has high charge transfer rate but large silicon crystals with well defined facets grow after 30 min on initially deposited porous silicon, which has low charge transfer rate (reprinted from Ref. 22, ©2000, with permission from Elsevier Science)

Further, Fig. 17*a* and *b* indicates that if charged diamond clusters lose their charge to a substrate with a high CTR, they transform instantly into graphite clusters. The loss of diamond stability after losing charge was attributed to the loss of an electrical double layer at the surface of diamond clusters.[3,87] The electrical double layer can be formed on a dielectric diamond cluster while it cannot on a conducting graphite cluster.

On substrates with a high CTR, the charge is lost just before landing and the resultant neutral clusters deposit on the substrate like flocculation, resulting in a porous structure. On substrates with a low CTR, however, the charge is retained in the clusters during landing and clusters undergo highly compact and regular packing of three-dimensional self-assembly or colloidal crystallisation, resulting in dense films.

Figure 18 shows these aspects in silicon CVD.[22] After 3 min of silicon CVD with a nickel substrate, porous silicon deposited (Fig. 18*a*), while after 30 min, large crystalline silicon grew on the porous silicon (Fig. 18(*b*)). In the initial stage, the porous silicon deposited because of the high CTR of the nickel substrate. But after the nickel substrate has been covered with porous silicon with a low CTR, dense silicon particles can grow on the initially-deposited porous silicon. Therefore, in order for charged clusters to undergo a self-assembly process, the substrate should have a low CTR.

Effect of cluster size

According to the TCC,[3–5] small clusters undergo epitaxial recrystallisation, leading to high quality films. With increasing cluster size at the given substrate temperature, defects such as twins tend to form. Large clusters tend to maintain their orientation and deposit as secondary nuclei, leading to a cauliflower structure or a nanostructure. This conclusion was derived from the analysis of the microstructural evolution of diamond films, which depended on the processing conditions.[3–5]

For example, in the diamond CVD process using a gas mixture of methane and hydrogen, low methane concentration produces high quality diamond crystals with well defined facets. With increasing methane concentration, the number density of defects, such as twins or grain boundaries, increases. For high methane concentrations, a cauliflower-shaped or nanodiamond structure evolves. Epitaxial recrystallisation is favoured not only by the small size of clusters, but also by a high deposition temperature. For example, the quality of diamond films improves with increasing substrate temperature for the same methane concentration.

Direct experimental observation of such deposition behaviour by charged clusters is almost impossible, but the deposition behaviour by clusters can be studied systematically by molecular dynamics (MD) simulation. The reliability of MD simulation depends on the reliability of the interatomic potential. Molecular dynamics simulation based on the embedded atom method (EAM)[88,89] is known to provide reliable results, especially in face centred cubic (fcc) metals.

Gold crystalline clusters containing 321, 1055, and 1985 atoms were deposited on the (110) gold surface at the specified deposition temperature. The (110) views of 321, 1055, and 1985 atom clusters at 300 K after 320 ps deposition are shown in Fig. 19. In order to identify the initial location of the atoms in the cluster, a grey scale was used, and it was made to increase from the centre to the surface of the cluster. The 321 atom cluster underwent complete homoepitaxial recrystallisation (Fig. 19*a*). However, the 1055 atom cluster contained a {111} twin after deposition (Fig. 19*b*). Since the twin boundary has ABCBA stacking sequence, the twin is a Σ3 boundary. The simulation was repeated with several different initial cluster orientations selected at random, but a twin was always observed. Twin formation appears to be a general phenomenon for this cluster size and substrate temperature. On the other hand, the 1985 atom cluster formed grain boundaries (Fig. 19*c*).

The (110) views of the 321, 1055, and 1985 atom clusters at 1000 K after 320 ps deposition are shown in Fig. 20. At the substrate temperature of 1000 K, the morphology of the deposited clusters was largely changed with most atoms in epitaxial lattice positions. The deposited clusters were rearranged into a hemispherical shape with most cluster atoms being mixed with each other.

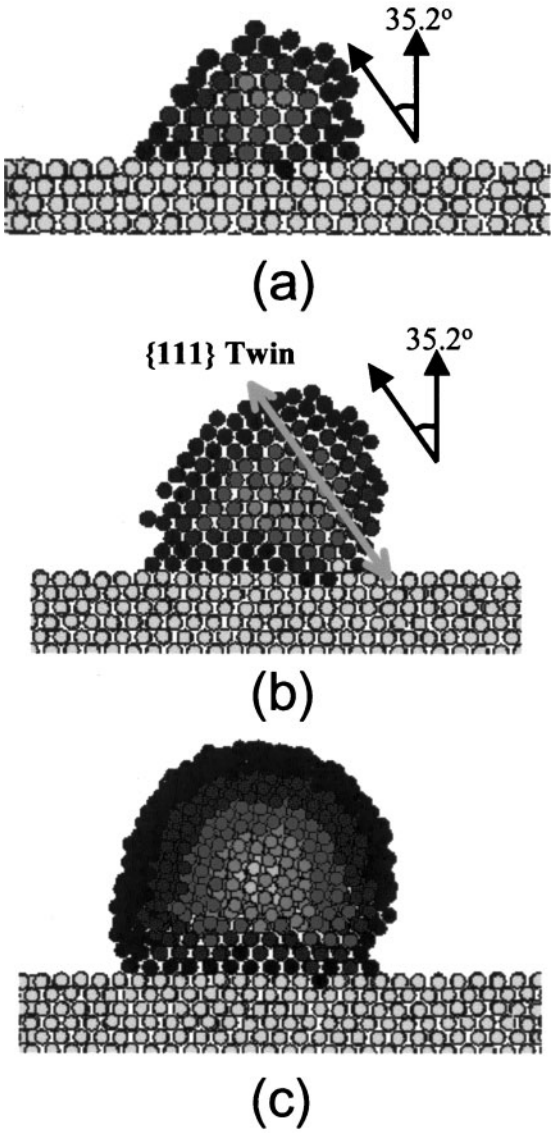

19 (110) plan views of *a* 321, *b* 1055, and *c* 1985 gold atom clusters after 320 ps of deposition by soft landing without any acceleration at 300 K: 321 atom cluster undergoes complete epitaxial recrystallisation, 1055 atom cluster produces (111) twin, and 1985 atom cluster produce grain boundaries (reprinted from Ref. 7, ©2002, with permission from Elsevier Science)

These simulation results indicate that epitaxial recrystallisation is favoured by small clusters and high deposition temperatures and secondary nucleation is favoured by large clusters and low deposition temperatures. By choosing the substrate with an appropriate lattice mismatch, the clusters can deposit as an epitaxial film if the cluster size is small and the deposition temperature is high. On the substrate with an inappropriate lattice mismatch, each cluster lands on the substrate with a non-epitaxial relation. Then, each cluster on the substrate would grow epitaxially with further cluster deposition, resulting in columnar growth. In this case, the grain size increases with deposition time.

When the cluster size is large and the deposition temperature is low, each cluster tends to maintain its orientation even after deposition, resulting in secondary nucleation. The grain size of films is determined by the ratio of the frequency of epitaxial recrystallisation to that of secondary nucleation. The grain size decreases with increasing frequency of secondary nucleation.

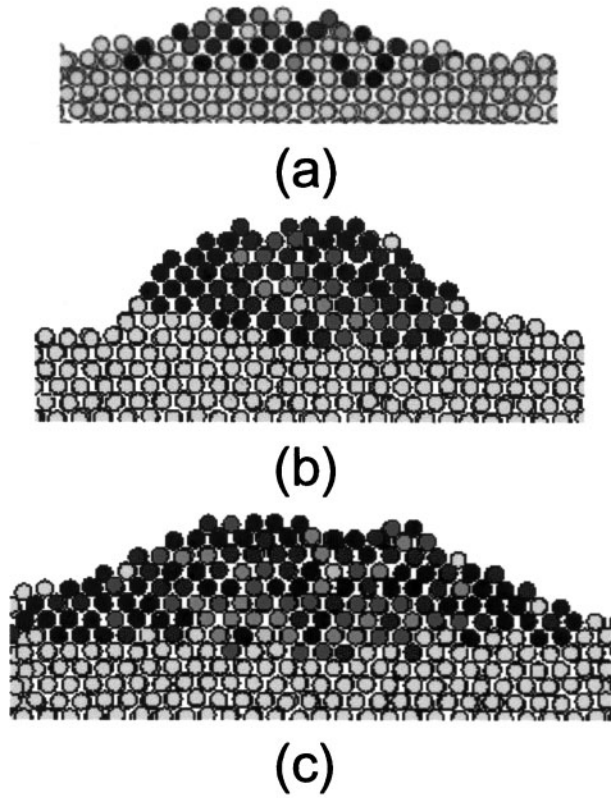

20 (110) plan views of *a* 321, *b* 1055, and *c* 1985 gold atom clusters after 320 ps of deposition at 1000 K: in this case, all clusters undergo epitaxial recrystallisation by soft landing without any acceleration (reprinted from Ref. 7, ©2002, with permission from Elsevier Science)

Deposition of amorphous phase

In the C–H system, positively charged carbon clusters tend to be hydrogenated, while negatively charged clusters are almost pure carbon.[86] Negatively charged clusters deposit as diamond films, while positively charged clusters deposit as graphitic carbon at high temperature, but as amorphous carbon at low temperature, which is attributed to the incomplete desorption of hydrogen. The hydrogen containing amorphous carbon, which is known as diamond-like carbon (DLC), is deposited by positively charged hydrogenated clusters.[5]

Similarly, in the silicon CVD process, positively charged silicon clusters appear to be hydrogenated and negatively charged clusters not hydrogenated. In thermal silicon CVD in the Si–H or Si–Cl–H system, positively charged hydrogenated silicon clusters are dominant. When these clusters are deposited at a substrate temperature high enough to desorb hydrogen, crystalline silicon will deposit. When the cluster size is small and the substrate temperature is high enough, the film grows epitaxially. When these clusters are deposited at a substrate temperature so low that the hydrogen cannot be sufficiently desorbed, amorphous silicon will deposit.[62]

In the thermal silicon CVD process, amorphous silicon is formed at deposition temperatures lower than ~853 K.[90] According to the new understanding of the TCC, the deposited amorphous silicon is attributed to the deposition of positively charged hydrogenated silicon clusters from which the hydrogen could not be desorbed at the low substrate temperature. Therefore, crystalline silicon films can be deposited at low temperatures if negatively charged silicon clusters are generated, which can be easily achieved by hot filament CVD.[62] Phenomenologically, it is well established that crystalline silicon can be deposited at low temperatures when hot wire CVD is used. The TCC provides the underlying principle as to why hot wire CVD can produce crystalline silicon at low temperatures. Low temperature deposition of crystalline silicon is important for solar cell and display technologies, and using the TCC provides a systematic way to develop this key technology.

When large hydrogenated clusters are deposited, the clusters will have a crystalline lattice structure surrounded by an amorphous layer. Films deposited by such clusters would show crystalline clusters embedded in an amorphous matrix. Such a microstructure is quite common in thin film processes, being called a microcrystalline or nanocrystalline structure.

Growth of nanowires or nanotubes by charged clusters

The selective deposition of charged clusters can lead to one-dimensional growth when charged clusters are attracted more strongly to the tip than to the sidewalls of the deposits. This type of deposition can produce nanowires, nanowhiskers, or nanotubes. One-dimensional growth is expected under the condition that the tip is more conducting than the sidewall. The tip is made conducting when a metal particle resides on it. Whisker growth of silicon using gold particles satisfies this condition.[91,92] Recently, silicon nanowires were fabricated by laser ablation.[93–96] Zhang *et al.*[95] suggested a cluster–solid mechanism for growth of silicon nanowires based on their observation that silicon nanoclusters had deposited on the cold finger during the growth of silicon nanowires by laser ablation.[95,97]

However, if these clusters are neutral, they will undergo rapid Brownian coagulation in the gas phase and produce fractal or skeletal structures. In order to explain the highly anisotropic one-dimensional growth of nanowires, the additional effect of charge should be considered. Zhang and co-workers[95,97] observed that a thin SiO_2 layer had formed on the outer surface of silicon nanowires. The insulating SiO_2 layer is expected to inhibit the attachment of charged silicon clusters on the sidewall and appears to induce the preferential attachment of clusters on the tip.

When two charged conducting spherical particles approach each other, the charge will move backwards in the clusters. In this case, the Coulomb interaction is described by the following equation[98]

$$F = \frac{q_1 q_2 e^2}{4\pi\varepsilon_o d^2} - \frac{q_1^2 e^2 r_2 d}{4\pi\varepsilon_o (d^2 - r_2^2)^2} - \frac{q_2^2 e^2 r_1 d}{4\pi\varepsilon_o (d^2 - r_1^2)^2} + \ldots \quad (5)$$

where the sphere of radius r_1 has a net charge q_1 and the sphere of radius r_2 has charge q_2; d is the distance between the centres, and $1/4\pi\varepsilon_o$ is the permittivity. The equation shows that the interaction changes from repulsion to attraction as the size difference between two clusters increases. For example, if $r_2 \gg r_1$ and thus $r_2 \approx d$, the interaction between the large and the small particles charged with the same sign can be attractive. In this case, the attraction will increase as q_2 increases. This analysis shows that the interaction between charged clusters of similar size tends to be repulsive, while that between small and large spheres can be less repulsive or even attractive.

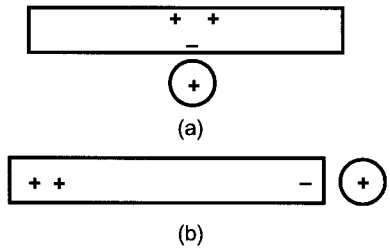

21 Coulomb interaction between rod and approaching spherical cluster (both of which are charged positively) is *a* repulsive when cluster approaches in radial direction of rod, but *b* attractive when cluster approaches in axial direction

A similar concept can be applied to the electrostatic interaction between an incoming charged cluster and a charged rod, as shown schematically in Fig. 21. When a positively charged cluster approaches the rod in the radial direction (Fig. 21*a*), the positive charge in the rod will be repelled to the opposite side of the rod. Since the repelled distance is not much, the electrostatic interaction would be repulsive. When a positively charged cluster approaches in the axial direction (Fig. 21*b*), however, the positive charge in the rod will be repelled much further away to the opposite end of the rod and the electrostatic interaction would be attractive. Thereby, charged clusters will be attached exclusively to the tip direction, leading to one-dimensional growth of nanowires.

Hwang *et al.* prepared silicon nanowires in a CVD process using SiH_4–HCl–H_2 gas mixtures.[99] The process was carried out at a substrate temperature of 1223 K under a pressure of 10 torr with a $SiH_4/HCl/H_2$ gas mixture ratio of 3 : 1 : 96. It should be noted that the SiH_4/HCl ratio is much higher than is usual in silicon CVD, for which it is generally 1 : 1 or 1 : 2. The higher ratio results in higher supersaturation of silicon and thereby in larger cluster size. According to the authors' experience, large charged clusters have less difficulty than small charged clusters in landing on an insulating surface. On a conducting substrate, nanowires did not grow, but typical silicon films deposited, as shown in Fig. 22*a*. On a silicon substrate, however, silicon nanowires started to grow after 3 min, as shown in Fig. 22*b*. The microstructure in Fig. 22*b* shows that the charged silicon clusters tend to deposit selectively on initially deposited silicon particles because of their relative difficulty in landing on the native silicon oxide formed on the silicon substrate. After 6 min of deposition, nanowires grew extensively on both silicon and SiO_2 substrates, as shown in Fig. 23*a* and *b* respectively.

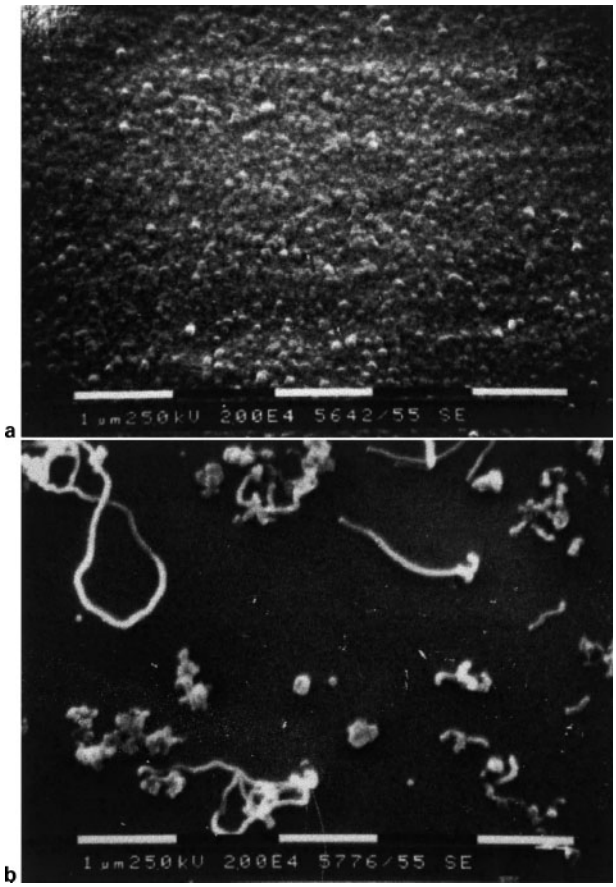

22 *a* Molybdenum and *b* silicon substrates after deposition for 3 min with gas mixture of $3SiH_4$–$1HCl$–$96H_2$ under pressure of 10 torr at substrate temperature of 1223 K: scale bar in each SEM represents 1 μm (reprinted from Ref. 99, ©2000, with permission from Elsevier Science)

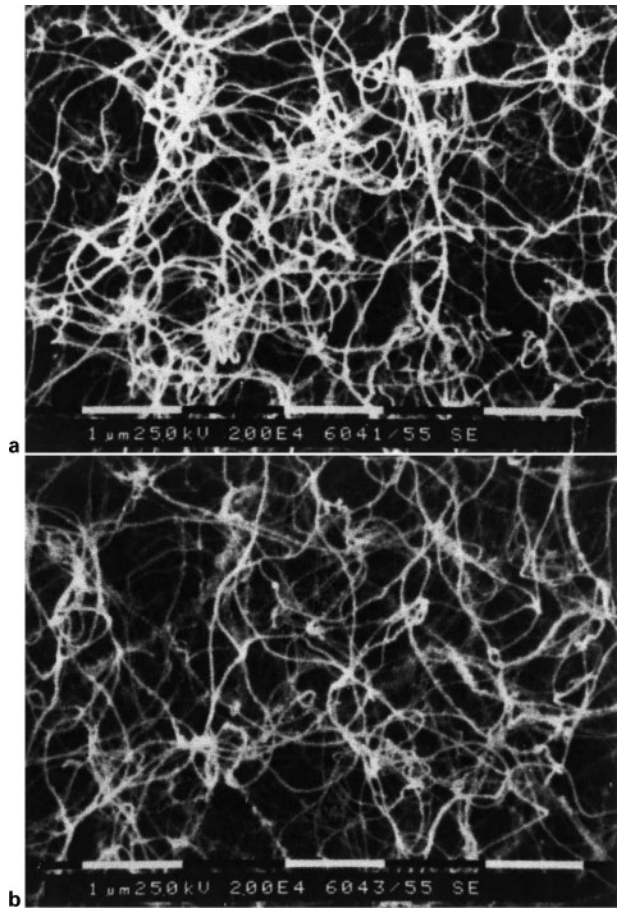

23 *a* Silicon and *b* silicon oxide substrates after deposition for 6 min with other conditions being same as those for Fig. 22 (scale bar in each SEM represents 1 μm): extensive growth of silicon nanowires occurred (reprinted from Ref. 99, ©2000, with permission from Elsevier Science)

It should be noted that materials with a high CTR such as iron and nickel are used to grow carbon nanotubes. In the present authors' laboratory, in hot filament diamond CVD experiments using substrates with a high CTR, carbon nanotubes were observed to grow in the later stage of soot growth just after ball-like diamonds started to grow on the soot. The formation of insulating diamonds appeared to be necessary for the growth of carbon nanotube for the repulsive interaction between charged clusters and the tube. Iron nanoparticles, which were originated from an iron substrate, were believed to assist the growth of carbon nanotubes. The typical microstructure is shown in Fig. 24. The specimen of Fig. 24 was prepared after deposition for 2 h with a $2CH_4$–$98H_2$ gas mixture under 20 torr with a distance of 8 mm between the filament and the iron substrate. The carbon nanotubes in Fig. 24 also grow by charged carbon clusters, the existence of which was experimentally confirmed in Figs. 3 and 4.

One-dimensional growth of carbon nanotubes comes from two factors. One is the Coulomb repulsion of charged carbon clusters when they approach the nanotubes in the radial direction. The other is highly selective landing of charged clusters on the catalytic materials of iron and nickel, to which charge is lost from the clusters. It should be noted that in the processing conditions of carbon nanotubes, methane concentrations are usually much higher than those used in the diamond CVD process and therefore charged carbon clusters are expected to form and to be involved in the growth of carbon nanotubes.

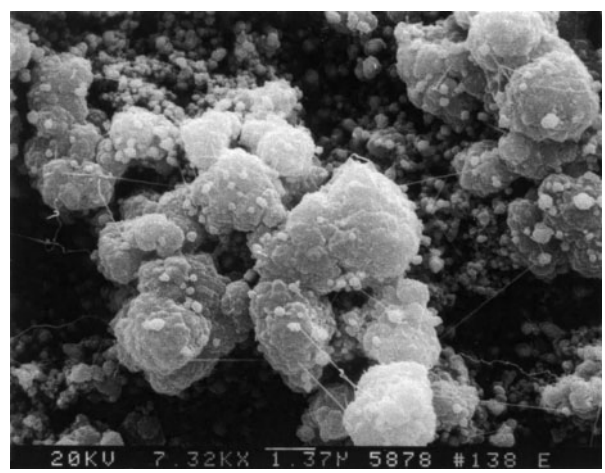

24 Carbon nanotubes, which grew on initially formed graphitic soot on iron substrate (SEM, scale bar represents 1·37 μm): growth unit must be charged carbon cluster because it has been experimentally confirmed that charged carbon clusters are generated under similar processing conditions[16,17]

Generation of charged clusters during crystal growth in solution

Crystal growth by clusters in solution has been systematically studied by Glasner and co-workers.[36–39,100] During crystal growth of KBr and KCl in an aqueous solution with Pb^{2+}, Glasner and Kenet[37] realised that nanometre sized nuclei were first formed in the solution and then became a growth unit. The formation of the nanometre sized clusters was confirmed by measuring the heat generated during precipitation. They demonstrated that a near perfect crystal could grow by orderly packing or self-assembly of the nanosized nuclei. The cluster size decreased with increasing concentration of Pb^{2+}. And with decreasing cluster size, the crystalline quality increased and the kinetics of crystallisation decreased. Small clusters crystallised into a transparent crystal, while large clusters crystallised into an opaque crystal.

Sunagawa[31,32] made a similar suggestion that the growth unit of synthetic diamond is not an atom but a much larger unit. According to the periodic bond chain (PBC) analysis of Hartman,[101] the (111), (110), and (100) plane surfaces of diamond are flat (F), stepped (S), and kinked (K) faces, respectively. The growth morphology of diamond by atomic deposition should be an octahedron surrounded by the slowest growing (111) planes. All natural diamonds satisfy this morphology predicted by PBC analysis. Synthetic diamonds produced either by a high pressure process or by a low pressure process are characterised by frequent evolution of the (110) or (100) surfaces, resulting in truncated octahedron or cubic shapes. Besides, the macrosteps of synthetic diamonds are wavy instead of being straight. Based on these observations, Sunagawa suggested that although the growth unit of natural diamonds is an atom, the growth unit of synthetic diamonds is much larger than individual atoms. He further presumed that the size of the growth unit would be comparable to the height of the wavy macrosteps.

There have been many reports on the existence of clusters in supersaturated solutions.[40,102–107] However, only a few reports mentioned that crystals grow by these clusters. Ueda *et al.*[40] suggested that the crystallisation of citric acid monohydrate proceeds not through a molecule-by-molecule process, but by an aggregation process of solute cluster units of size $\sim$60 nm. If these clusters in the supersaturated solution are neutral, they will grow instantly to visible size by Brownian coagulation. They must be electrically charged. The electrostatic repulsion between clusters in solution is the necessary condition for colloidal crystallisation by self-assembly.

The morphology of growth by monomers has been modelled by periodic bond chain (PBC) analysis by Hartman and Perdock.[108] If crystals grow not by monomers but by clusters, the growth shape will depend on the cluster size, which will depend on the processing parameters such as supersaturation. The morphology of growth by clusters in solution was analysed by Barber and Petty[109,110] based on moments of momenta (MoM) for dimer, trimer, tetramer, and so on. The MoM depend on the nature of the solution, while the PBC approach is controlled by the properties of the solid or crystal. The changes in crystal habit that accompany changes in solution, can be best explained by MoM analysis. It should be noted that if the growth shape depends on the cluster size, the textural evolution of the film should depend on the cluster size.

Even though there has been no systematic study as to the possibility of cluster growth in electrodeposition, cauliflower-shaped nanostructures are frequently evolved especially when some additives are used.[111] As further evidence, the textural evolution of films is affected sensitively by the processing conditions of the electrodeposition.[112]

Concluding remarks

While it has been generally accepted that thin films grow by the deposition of individual atoms or molecules, thin films are suggested to grow more generally by the deposition of charged clusters. The fact that thin films grow by self-assembly of charged clusters is not only important in basic science, but also provides critical guidelines to overcome technical breakthroughs in the synthesis of thin films, nanowires, quantum dots, and nanopowders. Although this review focuses on the theory of charged clusters in the thin film process, it must also be an important mechanism in many cases of solution growth.

Acknowledgements

This work was supported by the Creative Research Initiatives Program of the Korean Ministry of Science and Technology and by the Asian Office of Aerospace Research and Development (AOARD).

References

1. P. Bennema and G. H. Gilmer: in 'Crystal growth: an introduction', (ed. P. Hartman), 263–327; 1973, Amsterdam, North-Holland.
2. J. P. van der Eerden: in 'Handbook of crystal growth', Vol. 1: 'Fundamentals', Part A: 'Thermodynamics and kinetics', (ed. D. T. J. Hurle), 307–479, 1993, Amsterdam, North-Holland.
3. N. M. Hwang, J. H. Hahn and D. Y. Yoon: *J. Cryst. Growth*, 1996, **162**, 55–68.
4. N. M. Hwang: *J. Cryst. Growth*, 1999, **198–199**, 945–950.
5. N. M. Hwang, I. D. Jeon and D. Y. Kim: in 'Ceramic interfaces 2', (ed. H. I. Yoo and S. J. L. Kang), 85–109; 2001, London, The Institute of Materials.
6. K. H. Kingdon and I. Langmuir: *Phys. Rev.*, 1923, **21**, 380.
7. S. C. Lee, B. D. Yu, D. Y. Kim and N. M. Hwang: *J. Cryst. Growth*, 2002, **242**, 463–470.
8. I. Langmuir and K. H. Kingdon: *Proc. R. Soc. (London), Series A*, 1925, **107**, 61.
9. J. G. Wilson: 'The principles of cloud-chamber technique', 1–50; 1951, Cambridge, Cambridge University Press.
10. H. M. Jang and N. M. Hwang: *J. Mater. Res.*, 1998, **13**, 3527–3535.
11. M. C. Barnes, I. D. Jeon, D. Y. Kim and N. M. Hwang: *J. Cryst. Growth*, 2002, **242**, 455–462.
12. I. D. Jeon, M. C. Barnes, D. Y. Kim and N. M. Hwang: *J. Cryst. Growth*, 2003, **247**, 623–630.
13. N. M. Hwang and D. Y. Yoon: *J. Cryst. Growth*, 1996, **160**, 98–103.
14. N. M. Hwang, J. H. Hahn and D. Y. Yoon: *J. Cryst. Growth*, 1996, **160**, 87–97.
15. W. A. Yarbrough: *J. Am. Ceram. Soc.*, 1992, **75**, 3179–3200.
16. I. D. Jeon, C. J. Park, D. Y. Kim and N. M. Hwang: *J. Cryst. Growth*, 2000, **213**, 79–82.
17. I. D. Jeon, C. J. Park, D. Y. Kim and N. M. Hwang: *J. Cryst. Growth*, 2001, **223**, 6–14.
18. H. S. Ahn, H. M. Park, D. Y. Kim and N. M. Hwang: *J. Cryst. Growth*, 2002, **234**, 399–403.
19. N. M. Hwang: *J. Cryst. Growth*, 1999, **205**, 59–63.

20. N. M. Hwang, W. S. Cheong and D. Y. Yoon: *J. Cryst. Growth*, 1999, **206**, 177–186.
21. W. S. Cheong, N. M. Hwang and D. Y. Yoon: *J. Cryst. Growth*, 1999, **204**, 52–61.
22. W. S. Cheong, D. Y. Yoon, D. Y. Kim and N. M. Hwang: *J. Cryst. Growth*, 2000, **218**, 27–32.
23. I. D. Jeon, L. Gueroudji and N. M. Hwang: *Korean J. Ceram.*, 1999, **5**, 131–136.
24. I. D. Jeon, L. Gueroudji, D. Y. Kim and N. M. Hwang: *J. Korean Ceram. Soc.*, 2001, **38**, 218–224.
25. M. C. Barnes, D. Y. Kim, H. S. Ahn, C. O. Lee and N. M. Hwang: *J. Cryst. Growth*, 2000, **213**, 83–92.
26. B. S. Lee, M. C. Barnes, D. Y. Kim and N. M. Hwang: *J. Cryst. Growth*, 2002, **234**, 599–602.
27. M. Adachi, K. Okuyama, N. Tohge, M. Shimada, J. Sato and M. Muroyama: *Jpn J. Appl. Phys.*, 1992, **31**, L1439–L1442.
28. M. Adachi, K. Okuyama, N. Tohge, M. Shimada, J. Sato and M. Muroyama: *Jpn J. Appl. Phys.*, 1993, **32**, L748–L751.
29. M. Adachi, K. Okuyama and N. Tohge: *J. Mater. Sci.*, 1995, **30**, 932–937.
30. M. Adachi, K. Okuyama, T. Fujimoto, J. Sato and M. Muroyama: *Jpn J. Appl. Phys.*, 1996, **35**, 4438–4443.
31. I. Sunagawa: in 'Morphology of minerals', (ed. I. Sunagawa), 509–587; 1987, Tokyo, Terra Sci. Pub.
32. I. Sunagawa: *J. Cryst. Growth*, 1990, **99**, 1156–1161.
33. N. D. Samotoin: *Dokl. Earth Sci.*, 2001, **381**, 925–928.
34. Y. Takamura, N. Yamaguchi, K. Terashima and T. Yoshida: *J. Appl. Phys.*, 1998, **84**, 5084–5088.
35. Y. Takamura, K. Hayasaki, K. Terashima and T. Yoshida: *J. Vac. Sci. Technol. B*, 1997, **15**, 558–565.
36. A. Glasner and S. Skurnik: *Israel J. Chem.*, 1968, **6**, 69–72.
37. A. Glasner and J. Kenat: *J. Cryst. Growth*, 1968, **2**, 119–127.
38. A. Glasner and M. Tassa: *Israel J. Chem.*, 1974, **12**, 817–826.
39. A. Glasner and M. Tassa: *Israel J. Chem.*, 1974, **12**, 799–816.
40. M. Ueda, N. Hirokawa, Y. Harano, M. Moritoki and K. Ohgaki: *J. Cryst. Growth*, 1995, **156**, 261–266.
41. B. V. Derjaguin and D. B. Fedoseev: 'The growth of diamond and graphite from the gas phase'; 1977, Moscow, Nauka.
42. B. V. Spitsyn, L. L. Bouilov and B. V. Derjaguin: *J. Cryst. Growth*, 1981, **52**, 219–226.
43. S. Matsumoto, Y. Sato, M. Tsutumi and N. Setaka: *J. Mater. Sci.*, 1982, **17**, 3106–3112.
44. M. Kamo, Y. Sato, S. Matsumoto and N. Setaka: *J. Cryst. Growth*, 1983, **62**, 642–644.
45. J. C. Angus and C. C. Hayman: *Science*, 1988, **241**, 913–921.
46. K. E. Spear: *J. Am. Ceram. Soc.*, 1989, **72**, 171–191.
47. J. E. Butler, F. G. Celii, P. E. Pehrsson, H.-T. Wang and H. H. Nelson: in MRS. Symp. Proc., Vol. 131, 259–261; 1989, Warrendale, PA, Materials Research Society.
48. N. C. Angus, H. A. Will and W. S. Stanko: *J. Appl. Phys.*, 1968, **39**, 2915–2922.
49. A. R. Badzian, T. Badzian, R. Roy, R. Messier and K. E. Spear: *Mater. Res. Bull.*, 1988, **23**, 531–548.
50. M. C. Salvadori, M. A. Brewer, J. W. Ager, K. M. Krishnan and I. G. Brown: *J. Electrochem. Soc.*, 1992, **139**, 558–560.
51. W. G. Eversole: Synthesis of Diamond: US Patent 3,030,188 (17 April 1962).
52. N. M. Hwang, I. D. Jeon and D. Y. Kim: *J. Ceram. Process. Res.*, 2000, **1**, 34–44.
53. K. T. Whitby and B. Y. H. Liu: in 'Aerosol science', (ed. C. N. Davies); 1966, New York, Academic Press.
54. K. H. Homann and J. Traube: *Ber. Bunsenges. Phys. Chem.*, 1987, **91**, 828–833.
55. P. Gerhardt and K. H. Homann: *Combust. Flame*, 1990, **81**, 289–303.
56. P. Gerhardt and K. H. Homann: *J. Phys. Chem.*, 1990, **94**, 5381–5391.
57. R. Wegert, W. Wiese and K. H. Homann: *Combust. Flame*, 1993, **95**, 61–75.
58. P. K. Bachmann, D. Leers and H. Lydtin: *Diam. Relat. Mater.*, 1991, **1**, 1–12.
59. Y. Hirose, S. Amanuma and K. Komaki: *J. Appl. Phys.*, 1990, **68**, 6401–6405.
60. K. Hirabayashi, T. Kimura and Y. Hirose: *Appl. Phys. Lett.*, 1993, **62**, 354–356.
61. P. Gerhardt, S. Loffler and K. H. Homann: *Chem. Phys. Lett.*, 1987, **137**, 306–310.
62. J. Y. Kim: 'Chemical vapor deposition of low temperature poly-Si thin film by hot filament method', MS thesis, School of Materials Science and Engineering, Seoul National University, 2003.
63. H. Kumomi, T. Yonehara, Y. Nishigaki and N. Sato: *Appl. Surf. Sci.*, 1989, **41–42**, 638–642.
64. H. Kumomi and T. Yonehara: in MRS. Symp. Proc., Vol. 202, 83–88; 1991, Warrendale, PA, Materials Research Society.
65. H. Kumomi and T. Yonehara: *Jpn J. Appl. Phys.*, 1997, **36**, 1383–1388.
66. A. Wucher and M. Wahl: *Nucl. Instr. Methods B*, 1996, **102**, 581–589.
67. C. Staudt, R. Heinrich and A. Wucher: *Nucl. Instr. Methods B*, 2000, **164–165**, 677–686.
68. D. B. Chrisey and G. K. Hubler: 'Pulsed laser deposition of thin films'; 1994, New York, John Wiley.
69. B. S. Lee: 'Spontaneous formation of charged clusters during thermal evaporation of metals', MS thesis, School of Materials Science and Engineering, Seoul National University, 2000.
70. D. R. Lide: 'CRC handbook of chemistry and physics', 71st edn, 5-70, 10-211, 12-97–12-98; 1990–1991, Boca Raton, FL, CRC Press.
71. J. L. Persson, M. Andersson, L. Holmgren, T. Aklint and A. Rosen: *Chem. Phys. Lett.*, 1997, **271**, 61–66.
72. H. E. Stanley: 'Form: an introduction to self-similarity and fractal behavior', 21–53; 1986, Dordrecht, Martinus Nijhoff.
73. K. Tsubouchi and K. Masu: *J. Vac. Sci. Technol. A*, 1992, **10**, 856–862.
74. W.-K. Yeh, M.-C. Chen, P.-J. Wang, L.-M. Liu and M.-S. Lin: *Thin Solid Films*, 1995, **270**, 462–466.
75. P. G. Roberts, D. K. Milne, P. John, M. G. Jubber and J. I. B. Wilson: *J. Mater. Res.*, 1996, **11**, 3128–3132.
76. Y. Gao and J. H. Edgar: *J. Electrochem. Soc.*, 1997, **144**, 1875–1880.
77. T. T. Kodas and M. J. Hampden-Smith: 'The chemistry of metal CVD', 530; 1994, Weinheim, VCH.
78. J. O. M. Bockris and A. K. N. Reddy: 'Modern electrochemisry', 35; 1970, New York, Plenum Press.
79. J. M. Huh: 'Mechanism of soot formation on Ni, Fe, Co and Pd substrates and morphology variation of diamond with deposition conditions in CVD of diamond', MS thesis, Department of Materials Science and Engineering, Korea Advanced Institute of Science and Technology, 1994.
80. D. N. Belton and S. J. Schmieg: *Thin Solid Films*, 1992, **212**, 68–80.
81. J. W. Kim: 'The nucleation behaviour of diamond during gas phase synthesis', PhD thesis, Materials Science and Engineering, Korea Advanced Institute of Science and Technology, 1992.
82. K. Nishimura, K. Kobashi, Y. Kawater and T. Horiuchi: *Kobelco Technol. Rev.*, 1987, **2**, 49–52.
83. K. Kobashi, K. Nishimura, Y. Kawater and T. Horiuchi: *Phys. Rev. B*, 1988, **38**, 4067–4084.
84. C. R. Eddy, D. L. Youchison, B. D. Sartwell and K. S. Grabowski: *J. Mater. Res.*, 1992, **7**, 3255–3259.
85. Y. Mori, M. Deguchi, M. Kitabatake, H. Yagi, A. Hatta, T. Ito, T. Hirao and A. Hiraki: in *Proc. SPIE*, 1992, 18.
86. K. H. Homann and H. Wolf: in 21st Int. Symp. on 'Combustion', 1013–1021; 1986, Pittsburgh, PA, The Combustion Institute.
87. H. M. Jang and N. M. Hwang: *J. Mater. Res.*, 1998, **13**, 3536–3549.
88. M. S. Daw and M. I. Baskes: *Phys. Rev. Lett.*, 1983, **50**, 1285–1288.
89. M. S. Daw, S. M. Foiles and M. I. Baskes: *Mater. Sci. Rep.*, 1993, **9**, 251–310.
90. H. O. Pierson: 'Handbook of chemical vapor deposition'; 1992, New Jersey, Noyes Publications.
91. R. S. Wagner and W. C. Ellis: *Appl. Phys. Lett.*, 1964, **4**, 89.
92. E. I. Givargizov: *J. Cryst. Growth*, 1975, **31**, 20–30.
93. A. M. Morales and C. M. Lieber: *Science*, 1998, **279**, 208–211.
94. D. P. Yu, Z. G. Bai, Y. Ding, Q. L. Hang, H. Z. Zhang, J. J. Wang, Y. H. Zou, W. Qian, G. C. Xiong, H. T. Zhou and S. Q. Feng: *Appl. Phys. Lett.*, 1998, **72**, 3458–3460.
95. Y. F. Zhang, Y. H. Tang, N. Wang, C. S. Lee, I. Bello and S. T. Lee: *J. Cryst. Growth*, 1999, **197**, 136–140.
96. G. Zhou, Z. Zhang and D. Yu: *J. Cryst. Growth*, 1999, **197**, 129–135.
97. Y. F. Zhang, Y. H. Tang, H. Y. Peng, N. Wang, C. S. Lee, I. Bello and S. T. Lee: *Appl. Phys. Lett.*, 1999, **75**, 1842–1844.
98. D. B. Dove: *J. Appl. Phys.*, 1964, **35**, 2785–2786.
99. N. M. Hwang, W. S. Cheong, D. Y. Yoon and D. Y. Kim: *J. Cryst. Growth*, 2000, **218**, 33–39.
100. A. Glasner and S. Skurnik: *J. Chem. Phys.*, 1967, **47**, 3687–3688.
101. P. Hartman: 'Crystal growth: an introduction', 367–402; 1973, Amsterdam, North-Holland.
102. K. Ohgaki, Y. Makihara, M. Morishita, M. Ueda and N. Hirokawa: *Chem. Eng. Sci.*, 1991, **46**, 3283–3287.
103. K. Ohgaki, N. Hirokawa and M. Ueda: *Chem. Eng. Sci.*, 1992, **47**, 1819–1823.

104. S. Kim, A. S. Myerson and M. Kohl: *J. Cryst. Growth*, 1997, **181**, 61–69.
105. M. Bohenek, A. S. Myerson and W. M. Sun: *J. Cryst. Growth*, 1997, **179**, 213–225.
106. S. Devarakonda, A. Groysman and A. S. Myerson: *J. Cryst. Growth*, 1999, **204**, 525–538.
107. R. Mohan, O. Kaytancioglu and A. S. Myerson: *J. Cryst. Growth*, 2000, **217**, 393–403.
108. P. Hartman and W. G. Perdok: *Acta Crystallogr.*, 1955, **8**, 49–52.
109. P. G. Barber and J. T. Petty: *J. Cryst. Growth*, 1990, **100**, 185–188.
110. P. G. Barber: *J. Cryst. Growth*, 1991, **109**, 99–106.
111. C. Lingk and M. E. Gross: *J. Appl. Phys.*, 1998, **84**, 5547–53.
112. D. N. Lee: *Mater. Sci. Forum*, 2002, **408–412**, 75–94.